Dear Roland Bol,

below we provide first a point-by-point reply to the comments by referee #1 and we then summarise other corrections done since the original submission of the manuscript.

Point-by-point reply to the comments by referee #1
(Lines refer to original submitted manuscript)

1. Comment: It would be nice that the authors could give a schematic figure showing Mg fluxes in the studied system with respective delta values, fractions, flow strength, etc.

1. Reply: We added a schematic figure that illustrates the most important fluxes used in the manuscript.

2. Comment: There are many notations and symbols. I found it difficult to remember all of them while reading and had to go back to the text to look for them for the definition. So I recommend to make a list of the notations, providing necessary information, such as definition, link to the section, etc., similar in Bouchez et al., (2013).

2. Reply: We added a table that includes symbols and short descriptions of the variables used throughout the manuscript as in Bouchez et al. 2013. This table supports the additional schematic figure (see comment 1).

3. Comment: Repetition: page 5 line 145: The abundance of ... of XRD.

3. Reply: We removed this sentence as it is a repetition from line 142.

4. Comment: Typo: page 8 line 220: Section 4.9 instead of 3.9.

4. Reply: The typo was corrected as suggested.

5. Comment: Equation 2. is generally hard for me to understand, why deltaMg of creek water (deltaMg_diss) is used? How it is comparable with the closed system in Black et al. (2008)? Shouldn't the calculation of fraction (given % as in the manuscript) be based on mass fraction rather than delta values? Similar question is raised for Eq. 4.

5. Reply: Both equations (2) and (4) stem from mass balance models for the interpretation of isotope data, and thus relate isotope ratios to relative fluxes / mass fractions. Equation (2) is a mass balance equation frequently used in stable isotope geochemistry to calculate the partitioning of an element into two distinct compartments in a "closed system" (meaning one in which the element can freely exchange between two compartments, with no external inputs to or outputs from these two compartments). Equation (4) is derived from Bouchez et al. 2013 (where the considered system is an "open flow through box model" representing the weathering zone) and expresses this compartment separation in terms of relative fluxes. To make this clearer, we have slightly rewritten section 4.2.

In contrast, equations (5) to (8) and (12) use measured fluxes to calculate how relative mass fractions of elements partition within an ecosystem. The accurate measure of these fluxes requires long-term monitoring programs, which are cost-intensive and time-consuming and hence not always available. However, in our field site (part of a "Critical Zone Observatory") these fluxes have been determined. The novel approach of our manuscript is thus to compare these metrics to those derived from stable isotope measurements, in order to establish methods that avoid the necessity of data from long-term

monitoring programs. Therefore, we show that the Mg flux fractions in an ecosystem can be quantified by isotope analyses with much less effort.

6. Comment: page 7 line 187-188: The combination of ... to the transient growth of biomass. Please explain.
6. Reply: For using mass balance equations based on isotopes it is important to clarify under which conditions they can be applied; e.g. steady state of all or some of the considered compartments. The equation involving the two rightmost terms of equation (3) does not require that the biomass and plant litter compartments are at steady state: if there is net biomass Mg increase in the ecosystem the associated Mg uptake into plants would be accurately quantified with this equation. However, for these two terms to be equal to the leftmost term in equation (3), another condition has to be matched: the biomass and the litter Mg pools have to be at steady state. To clarify this point, we have rewritten section 4.2, and split equation (3) into two equations (one valid even out of steady biomass + litter Mg, the second valid only for steady state conditions).

7. Comment: Typo: page 10 line 293: Sect. 4.3 instead of 3.3
7. Reply: The typo has been corrected.

8. Comment: sect. 4.6, Na is a nutrient, why not taken up by plants, as indicated on page 11 line 304-305? The percentage of those elements in streams dissolved load should be re-considered.
8. Reply: Generally, Na can be considered as a beneficial element in halophylic and C4/CAM plants (Marschner et al. 2011) and in plants that are under K deficient conditions (Pilon-Smits et al. 2009). Since the main tree species at SSCZO are pine trees, we argue that Na plays no significant nutritive role. Moreover, we determined the fraction of Na taken up by trees at SSCZO from published litter fall data and find that only 2 % of Na once released by chemical weathering is taken up by forest trees. Therefore, values of the DEF^{X} (renamed to $\mathbf{DEE}_{\mathbf{Na}}^{\mathbf{X}}$ (dissolved export efficiency) in the revised manuscript), which is the only metric where Na is used for normalisation, are assumed not to be affected by Na uptake which in any case would be minor. To clarify this, we added text to section 4.6.

9. Comment: page 11 line 309, such as and for example are repetition
9. Reply: The repetition "for example" has been removed.

10. Comment: line 318: ... by chemical weathering that results in ...
10. Reply: The typo has been corrected as suggested.

11. Comment: Sect 4.7, if 60% K solubilized from rock is in the streams dissolved load, how K is relatively highly recycled compared with other elements studied? What the relation between DEF and Rec?
11. Reply: The DEF^{X} (renamed to $\mathbf{DEE}_{\mathbf{Na}}^{\mathbf{X}}$ (dissolved export efficiency) in the revised manuscript) and the Rec^{X} are fully independent from each other. This independency arises because an element X can become recycled (meaning uptake of nutrients released from plant litter) many times compared to this element's weathering flux (formerly $\mathbf{W}_{\tau}^{\mathbf{X}}$, renamed to $\mathbf{W}_{\mathbf{regolith}}^{\mathbf{X}}$ in the revised manuscript). This number of cycles is quantified by Rec^{X}. In contrast, $\mathbf{DEE}_{\mathbf{Na}}^{\mathbf{X}}$ quantifies the fraction of an element X that is lost from the ecosystem in the dissolved river load relative to the fraction of X that was initially solubilised by chemical weathering. Thus (if there are no atmospheric inputs) $\mathbf{DEE}_{\mathbf{Na}}^{\mathbf{X}}$ can vary only between 0 and 1, whereas Rec^{X} can vary between 0 and a large number. To clarify these relations, we added text to and rephrased sentences in section 4.7.

12. Comment: Fig. B1 is not very high quality, may be replaced by above mentioned schematic of the fluxes in the system.

12. Reply: We improved the resolution of figure B1 by rearranging figure B1. Additionally, we added a schematic figure (see comment 1).

References cited in the point-by-point reply to the comments by referee #1

Aciego, S. M., Riebe, C. S., Hart, S. C., Blakowski, M. A., Carey, C. J., Aarons, S. M., Dove, N. C., Botthoff, J. K., Sims, K. W. W. and Aronson, E. L: Dust outpaces bedrock in nutrient supply to montane forest ecosystems, Nat. Commun., 8, 14800, 2017.

Bouchez, J., von Blanckenburg, F. and Schuessler, J. A.: Modelling novel stable isotopes in the weathering zone, Am. J. Sci., 313, 267-308, 2013.

Marschner, H. (2011). Marschner's mineral nutrition of higher plants. Academic press.

Pilon-Smits, E. A., Quinn, C. F., Tapken, W., Malagoli, M., & Schiavon, M. (2009). Physiological functions of beneficial elements. Current opinion in plant biology, 12(3), 267-274.

<u>Other corrections that have been done since the original submission of the manuscript</u>
(sorted after sections)

- Abstract:
    - For better understanding, we added text and rephrased sentences (see revision marks).
    - The typo concerning the nutrient uptake depth (6 m instead of 7 m (where 7 m is the depth of the weathering profile)) has been corrected.
- 1 Introduction:
    - We removed the citation Dixon et al. 2009 as the definition of regolith is general and does not need a citation.
    - We replaced the word “mineralisation” by more specific phrases as “mineralisation” is defined differently in different scientific communities.
    - We added the citation Bullen and Chadwick 2016 as nutrient uplift of P is addressed in this paper too.
    - We added the citation Marschner et al. 2011 as it defines nutrients into macronutrients, micronutrients and plant beneficial elements.
    - For better understanding, we added text and rephrased sentences (see revision marks).
- 2.1 Study site
    - We moved the last sentence here where it fits better.
    - We added text as we became aware of the paper by Aciego et al. 2017 which addresses P input by dust deposition in much more detail as known at the time of the original submission of the manuscript.
- 2.2 Analytical methods
    - We corrected the cross reference of the tables.
- 2.3 Mg isotope analyses by MC-ICP-MS
    - Same correction as in section 2.2.

- 2.4 Mg isotope analyses by fsLA-MC-ICP-MS
    - Minor technical corrections.
- 3.1 Mg isotopic composition of ecosystem compartments
    - We corrected the numbers of the cross references of the supplementary tables.
- 4.1 Mg isotopic fractionation by clay formation
    - For better understanding, we added text and rephrased sentences (see revision marks).
    - We corrected the numbers of the cross references of the supplementary tables.
- 4.2 Mg tree uptake fractions from an isotope mass balance
    - See above to the reply to comments 5 and 6 by referee #1.
    - For more clarity regarding a system at steady state and a system in transience, and regarding the split of equation (3) into two equations, we added and rephrased text (see revision marks).
    - We corrected the numbers of the cross references of figures, equations, sections and the subscript in E^{Mg} to E_{org}^{Mg}.
- 4.3 Mg weathering fluxes from an isotope mass balance
    - We replaced the subscript "iso" in w_{iso}^{X} with "isotope" ($w_{isotope}^{X}$) which provides more clarity in definitions.
    - We also recalculated $w_{isotope}^{X}$ as we use the mean of δ^{26}Mg from bulk soil and bulk saprolite instead of topsoil only. The recalculation was done as soil and saprolite samples vary insignificantly in their δ^{26}Mg and the mean value is a more representative estimate of δ^{26}Mg of exported particulate matter (where topsoil is the compartment that is undergoing erosion at our sites). The recalculated values differ insignificantly to the values before and have been added to table S4b.
    - We removed the argumentation why we only measured Mg stable isotopes but not the isotopes of the other bio-elements, which we considered not necessary.
    - We corrected the numbers of figures, equations and supplementary tables.
    - For better understanding, we slightly rephrased sentences (see revision marks).
    - We corrected the numbers in the cross references of figures, equations and supplementary tables.
- 4.4 Elemental dissolved river fluxes
    - We replaced the subscript "diss" in W_{diss}^{X}, w_{diss}^{X} and $[X]_{diss}$ with the subscript "river". (W_{river}^{X}, w_{river}^{X}, $[X]_{river}$) throughout the revised manuscript This was done as "diss" suggests that an element becomes dissolved. However we refer to what is exported in the dissolved river loads.
    - For better understanding, we added a definition of the word "bio-elements".
    - We replaced the unit "t km^{-2} yr^{-1}" into "mol km^{-2} yr^{-1}" as it was a typo before.
    - We corrected the sampling years as it was a typo before.
    - For better understanding, we slightly rephrased sentences (see revision marks).
    - We corrected the numbers of the cross references of figures and equations.
- 4.5 Net elemental solubilisation fluxes in the weathering zone
    - We replaced the subscript "τ" in W_{τ}^{X} and w_{τ}^{X} with "regolith" ($W_{regolith}^{X}$, $w_{regolith}^{X}$) throughout the revised manuscript to be consistent with the nomenclature used in section 4.4 where "river" refers to the material it is based on.

  - We have recalculated $\mathrm{W}_{\mathrm{regolith}}^{\mathrm{X}}$ because τ^{P} of top mineral soil was used before. Since τ^{P} increases towards the Earth surface (due to nutrient uplift or dust deposition), we used the most negative τ^{P} at our three study sites from the data compilation from tables S3a - S3c instead. We also recalculated $\mathrm{Rec}^{\mathrm{P}}$ and $\mathrm{DEE}_{\mathrm{Na}}^{\mathrm{P}}$ (formerly $\mathrm{DEF}^{\mathrm{P}}$) as both rely on $\mathrm{W}_{\mathrm{regolith}}^{\mathrm{X}}$. Accordingly we corrected Fig. 5 (formerly Fig. 4) and tables S4a and S4f (formerly S4e).
  - We corrected equation (9) (formerly (8)) as RP^{X} was defined in section 4.4.
  - We corrected equation (10) (formerly (9)) for more clarity.
  - For better understanding, we slightly rephrased sentences (see revision marks).
  - We corrected the numbers of the cross references of figures, equations, supplementary tables and sections.
- 4.6 Dissolved export efficiency
  - We renamed the term “dissolved export fraction ($\mathrm{DEF}^{\mathrm{X}}$)” into “dissolved export efficiency ($\mathrm{DEE}^{\mathrm{X}}$)” throughout the manuscript as we express how efficient an element is exported from the headwater catchment in the dissolved form relative to its net solubilisation by chemical weathering.
  - We became aware that the Na-normalisation used to derive $\mathrm{DEE}_{\mathrm{Na}}^{\mathrm{X}}$ needs more motivation. Therefore we now first introduce the $\mathrm{DEE}^{\mathrm{X}}$ without Na-normalisation. Then we explain why the Na-normalisation is needed required (section 4.6). Accordingly we a) added equation (12), b) added $\mathrm{DEE}^{\mathrm{X}}$ into Fig. 6 (formerly Fig. 5), and c) added a supplementary table (S4d in the revised supplements). We also determined foliage, stem and root litter fall fluxes for Na to underpin that Na is no nutrient to the tree species at SSCZO and to quantify the tree uptake flux of Na relative to the net solubilisation flux ($\mathrm{W}_{\mathrm{regolith}}^{\mathrm{X}}$) by chemical weathering. Accordingly we added the $\mathrm{DEE}^{\mathrm{Na}}$ data to the new table S4d.
  - We corrected the numbers of the cross references of figures, equations and supplementary tables.
  - For better understanding, we slightly rephrased sentences (see revision marks).
- 4.7 Nutrient recycling factor
  - We moved the description of determining of the foliage, stem and root litter fall fluxes into the Appendix C as this paragraph contains method details that interrupt the flow of the main text.
  - We recalculated $\mathrm{Rec}^{\mathrm{P}}$ as we recalculated $\mathrm{W}_{\mathrm{regolith}}^{\mathrm{P}}$.
  - For better understanding, we rephrased sentences (see revision marks).
  - We added text (last paragraph) to address to the comments by referee #1 (comment 11, reply 11).
- 4.8 Accumulation of bio-elements during forest growth or export in coarse woody debris (CWD)?
  - We have become aware of the fact that the Providence Creek forest was managed up to the 1960s (in addition to having been wholesale clear cut at the end of the 19th century). Therefore, the forest biomass is likely still re-growing. This growth might accumulate the strongly bio-utilised elements and potentially provides an explanation for the partitioning of $^{26}\mathrm{Mg}$ over $^{24}\mathrm{Mg}$ in biomass. We corrected the heading of section 4.8, added text and rephrased sentences to explain this scenario as an additional mechanism to the one suggested in the original version of the submitted manuscript: erosional export of leaf litter, phytoliths, and coarse woody debris from the watershed. While the former

    mechanism might be in operation today, the latter might have been significant in pre-forest management times.
  - We became aware that $\mathrm{Rec}^{\mathrm{Si}}$ is extremely low (<0.1) but $\mathrm{DEE}_{\mathrm{Na}}^{\mathrm{Si}}$ not correspondingly high (0.5). To explain this contradiction, that we attribute to the difficulty in obtaining representative estimates for the recycled biosilica we added text.
  - We also rephrased text to improve the logical structure and for better understanding.
  - We corrected the numbers in the cross references of sections and typos in citations.
- 4.9 Nutrient uplift from the deep saprolite
  - We added the citation Bullen and Chadwick 2016 as a) nutrient uplift of P and b) the absence of isotopic fractionation during adsorption onto clay minerals of other bivalent cations are addressed in this paper too.
  - We improved slightly the English and corrected cross references of figures.
  - The typo concerning the nutrient uptake depth (6 m instead of 7 m (where 7 m is the depth of the weathering profile)) and spelling has been corrected.
- 5.0 Atmospheric depositional fluxes
  - This section has been added to explain in more detail (atmospheric dust deposition has been addressed only in a general sense in section “2.1 Study site”) the relevance of dust depositions at our study sites with respect to our new metrics.
- 6 Implications
  - We corrected the number of the section.
  - The typo concerning the nutrient uptake depth (6 m instead of 7 m (where 7 m is the depth of the weathering profile)) has been corrected.
  - For better understanding, we slightly rephrased some sentences (see revision marks).
  - We removed the citation “Brantley et al., 2011”in this section as it was inappropriate at this place and added the citation “Hilton, 2017” as we became aware of its publication since the original submission of this manuscript.
- 7 Conclusions
  - We corrected the number of the section and spelling (British English).
  - The typo concerning the nutrient uptake depth (6 m instead of 7 m (where 7 m is the depth of the weathering profile)) has been corrected.
  - We corrected values for $\mathrm{w}_{\mathrm{isotope}}^{\mathrm{Mg}}$ and $1\text{-}\mathrm{DEE}_{\mathrm{Na}}^{\mathrm{P}}$ as the metrics has been recalculated.
  - We added and (1-$\mathrm{DEE}_{\mathrm{Na}}^{X}$) for better understanding.
  - For better understanding we rephrased sentences (see revision marks).
  - We added text to account to the thinning and forest re-growth scenario.
- 8 Appendices
  - We corrected the number of the section
- Appendix A: Calculating δ^{26}Mg in bulk tree
  - We corrected punctuation and cross references of figures.
- Appendix B: X-ray diffraction analyses and the potential incorporation of Mg into secondary minerals
  - We corrected spelling and cross references of sections.
- Appendix C: Determining foliage, stem and root litter fall fluxes
  - We corrected the heading of this section.
  - We replaced text from section 4.7 into this section as this paragraph contains method details.

    - We added the element Na to the text as we determined the uptake flux of Na by forest trees in section 4.7.
- 9 Author contributions, 10 Competing financial interests, 11 Additional information
    - We corrected the numbers of the sections.
- 12 Acknowledgements
    - We corrected the number of the section and performed minor technical corrections.
    - We added D. Calmels as we acknowledge him for his comprehensive discussions.
- 13 References
    - We corrected the number of the section.
    - By reasons mentioned above we added the citations: Aciego et al., 2017; Bullen and Chadwick 2016; Hilton, 2017; Kirchner et al., 2001; Schaller et al., 2001
    - We removed the citations: Bolou-Bi et al., 2010 (not cited in main text), Fantle et al., 2014 (removed paragraph in main text), Mahowald et al., 2011 (replaced by Aciego et al., 2017), Opfergelt et al., 2012 (removed paragraph in main text), Wang et al., 2016 (removed paragraph in main text)
    - We corrected the citations: Chapela Lara et al., 2017 (published now)
- 14 Tables
    - We added this table as it was requested by referee#1 (comment and reply no. 2)
- 15. Figures
    - We corrected the number of the section and figures as we added one figure as requested by referee #1 (comment and reply no. 1)
    - We improved the design of Fig. 1.
    - We added the data of plant samples from the forest floor and the sediment pond into Fig. 3. This data was already discussed in section 4.2 and reported in table S2 in the original submitted version of the manuscript, but not shown in a figure. We also corrected the caption of Fig. 3.
    - We added Fig. 4 as requested by referee #1 (comment and reply no. 1).
    - We corrected Fig. 5 (formerly Fig. 4) and its captions as we recalculated $\mathrm{w}^{\mathrm{Mg}}_{\mathrm{isotope}}$ and as we corrected the subscripts of the metrics $\mathrm{w}^{\mathrm{X}}_{\mathrm{regolith}}$ and $\mathrm{w}^{\mathrm{X}}_{\mathrm{river}}$.
    - We corrected Fig. 6 (formerly Fig. 5) and its captions as we recalculated $\mathrm{Rec}^{\mathrm{P}}$, renamed $\mathrm{DEF}^{\mathrm{X}}$ and added the non Na-normalised metric $\mathrm{DEE}^{\mathrm{X}}$.
    - We improved the resolution of Fig. B1 as requested by referee #1 (comment and reply no. 12) by rearranging the design of the figure. We also corrected the caption of Fig. B1.
- Supplementary tables
    - We corrected values in tables S4a, S4b, S4e (formerly S4d) and S4f (formerly S4e) as we recalculated $\mathrm{w}^{\mathrm{Mg}}_{\mathrm{isotope,}}$ $\mathrm{W}^{\mathrm{P}}_{\mathrm{regolith}}$, $\mathrm{DEE}^{\mathrm{X}}_{\mathrm{Na}}$ and $\mathrm{Rec}^{\mathrm{X}}$.
    - We corrected values in Tab. S4c as we became aware that this table contained typos. The values changed only slightly so that interpretation is not affected.
    - We reformatted the data in tables S2, S4a and S4c by adding the thousands separator comma.
    - We also slightly reformatted all supplementary tables.
    - We added total biomass data of foliage, stem and root litter as well as elemental concentrations of foliage, stem and root litter that has been cited in the main text and is

used to calculate elemental litter fall fluxes. We added this data to facilitate the reader to reproduce our calculations.

- We added table S4d as we added the non Na-normalised DEE^X to section 4.6 and Fig. 6 (formerly Fig. 5) and corrected the numbers of the following supplementary tables.

Sincerely yours,
David Uhlig and co-authors

Quantifying nutrient uptake as driver of rock weathering in forest ecosystems by magnesium stable isotopes

David Uhlig[1], Jan A. Schuessler[1], Julien Bouchez[1,2], Jean L. Dixon[1,3], Friedhelm von Blanckenburg[1,4]

[1]GFZ German Research Centre for Geosciences, Earth Surface Geochemistry, Telegrafenberg, 14473 Potsdam, Germany
[2]Present address: IPGP-CNRS Institut de Physique du Globe de Paris, rue Jussieu, 75238 Paris cedex 05, France
[3]Present address: Montana State University, Department of Earth Sciences, Bozeman, Montana 59717, USA
[4]Freie Universität Berlin, Institute of Geological Sciences, Malteserstr. 74-100, 12249 Berlin, Germany

Correspondence to: David Uhlig (david.uhlig@gfz-potsdam.de)

Abstract Plants and soil microbiota play an active role in rock weathering and potentially couple weathering at depth with erosion at the soil surface. The nature of this coupling is still unresolved because we lacked means to quantify the passage of chemical elements from rock through higher plants. In a temperate forested landscape characterised by relatively fast (~220 t km^{-2} yr^{-1}) denudation and a kinetically-limited weathering regime of the Southern Sierra Critical Zone Observatory (SSCZO), California, we measured magnesium (Mg) stable isotopes that are sensitive indicators of Mg utilisation by biota. We find that Mg is highly bio-utilised: 50-100 % of the Mg released by chemical weathering is taken up by forest trees. To estimate the tree uptake of other bio-utilised elements (K, Ca, P and Si) we compared the dissolved fluxes of these elements and Mg in rivers with their solubilisation fluxes from rock (rock dissolution flux minus secondary mineral formation flux). We find a deficit in the dissolved fluxes throughout, that we attribute to the nutrient uptake by forest trees. Therefore both the Mg isotopes and the flux comparison suggests that a substantial part of the major element weathering flux is consumed by the tree biomass. The enrichment of ^{26}Mg over ^{24}Mg in tree trunks relative to leaves suggests that tree trunks account for a substantial fraction of the net uptake of Mg. This isotopic and elemental compartment separation is ~~preserved only if~~prevented from obliteration (which would occur by Mg redissolution) by two potential effects. Either the mineral nutrients ~~contained in~~accumulate today in regrowing forest biomass ~~are prevented from re-dissolution~~ after clear cutting, or they are exported in litter ~~fall, showing that these nutrients have been removed as "solid" biomass. The enrichment of ^{26}Mg over ^{24}Mg in tree trunks relative to leaf litter suggests that this removal occurs mainly in~~ and coarse woody debris (CWD~~). Today, CWD is exported from the ecosystem by tree logging.~~) such that they remain in "solid" biomass. Over pre-~~anthropogenic~~forest management weathering time scales, ~~a similar~~this removal flux might have been in operation in the form of natural erosion of CWD. Regardless of the removal mechanism, our ~~data~~approach provides ~~the first~~entirely novel means towards the direct quantification of biogenic uptake following weathering. We find that Mg and other nutrients and the plant-beneficial element Si ("bio-elements") are taken up by trees at up to ~~7~~ 6 m depth, and surface recycling of all bio-elements but P is minimal. Thus, in the watersheds of the SSCZO~~ in which weathering is fast and kinetically-limited~~, the coupling between erosion and weathering might be established by bio-elements that are taken up by trees, are not recycled and are missing in the dissolved river flux due to erosion as CWD and as leaf-derived bio-opal for Si. We suggest that the partitioning of a biogenic weathering flux into eroded plant

debris might represent a significant global contribution to element export after weathering in eroding mountain catchments that are characterised by a continuous supply of fresh mineral nutrients.

1 Introduction

In continuously eroding landscapes, the mass loss of particles by erosion and solutes by drainage needs to be balanced over a ~ kilo year time scale by the conversion of rock into regolith, where we define regolith as the entire weathering zone above bedrock, including topsoil~~ (Dixon and von Blanckenburg, 2012).~~. The advance of the weathering front at depth is thus coupled to surface denudation (Brantley and Lebeveda, 2011). It has been hypothesised that biotic processes contribute towards this coupling (Brantley et al., 2011). If the nutrient demand of plants and soil microbes is linked to the advance of the weathering front, investigating the dependence of nutrient fluxes on the weathering regime allows for a test of ~~the ~~this “biogenic weathering” hypothesis.

The way weathering systems operate can be characterised by two endmembers, each associated with a specific pattern of nutrient dynamics. In the supply-limited regime, the transfer of nutrient-bearing mineral grains from rock into the regolith is so slow that their complete dissolution ~~decreases~~makes the mineral nutrient status of the regolith ~~and~~very low, such that plants and soil microbes are rather nourished by ~~re-mineralisation and ~~recycling of nutrients extracted ~~-~~from plant litter (Lang et al., 2016; Vitousek and Farington, 1997) and by atmospheric inputs (Vitousek and Farington, 1997). In the kinetically-limited regime, ~~ongoing ~~erosion rejuvenates the regolith (Porder et al., 2007), such that the rate of supply outpaces the weathering of minerals (West et al., 2005). ~~The~~In the kinetically-limited system, the supply of solutes by chemical weathering into soil solutions ensures that nutrients are readily available for plant uptake from regolith water~~. In this regime of long-lasting erosion,~~, and a fraction of these nutrients is lost after bio-utilisation in plant debris such as leaf litter and coarse woody debris (CWD). The plant litter can also be “re-mineralised~~,~~” (meaning oxidation of plant litter), so that nutrients are lost by drainage in the dissolved form. If erosion of plant debris outpaces nutrient leaching, nutrients are eroded in leaf litter by erosion or stochastically as woody matter in landslides. To replace either loss, nutrients ~~are~~should be uplifted from subsoil layers (Jobbagy and Jackson, 2001; Bullen and Chadwick, 2016). To facilitate the uplift from subsoil in the kinetically-limited regime, plants and soil microbes ~~can~~could stimulate chemical weathering rates by decreasing the rhizospheric pH through respiration ~~of CO$_2$~~ and~~ the~~ excretion of weathering agents (Brantley et al., 2011). Moreover, the symbiosis of roots with mycorrhiza fungi (Landeweert et al., 2001) ~~enables~~could enable plants to directly assimilate nutrients from primary minerals (Jongmans et al., 1997). Here we explore this ~~hypothesis~~set of hypotheses in a kinetically-limited mountain setting using isotopic and geochemical techniques.

The stable isotopes of magnesium (Mg) - a macronutrient for plants (Marschner, 2011) and a major constituent of the bulk silicate Earth - are ~~suitable~~suited to trace these cycles. Unless ~~fractionated by ~~the ~~neoformation~~formation of secondary minerals is significant (Wimpenny et al., 2014), the main shift affecting the ^{26}Mg/^{24}Mg ratio ~~is mainly shifted~~in weathering systems is the isotopic fractionation towards high ~~values~~ratios during nutrient uptake by plants (Black et al., 2008; Bolou-Bi et al., 2012; Mavromatis et al., 2014), ~~and~~such that the residual dissolved Mg is shifted towards the complementary low ratio. These two isotopically distinct compartments will remain separated if a fraction of the Mg accumulates in wood of a regrowing forest after clear cutting, or if a fraction of the Mg is eroded ~~as mainly CWD~~ after utilisation and is not released back into solution. In that case the isotope ratio serves as a proxy for the catchment~~-~~-wide net nutrient uptake flux, where “net” excludes ~~re-mineralisation~~dissolution from biomass and recycling. Here we use an isotope mass balance model (Bouchez et al., 2013) to quantify ~~what~~ the relative fluxes ~~are that export~~of Mg transfer in the ecosystem after Mg release by rock weathering: uptake into plants, export as solute, or erosion in particles including minerals and a substantial CWD fraction at three forested headwater catchments.

2 Methods

2.1 Study site

Our study sites comprise three catchments at Providence Creek, Sierra Nevada, USA and are part of two monitoring programs: Kings River Experimental Watersheds (KREW) and Southern Sierra Critical Zone Observatory (SSCZO). The extensive ~~SSCZO~~monitoring dataset is highly suited for nutrient cycling studies in forest ecosystems and provides evidence that rock phosphorus (P) might be growth-limiting (Hahm et al., 2014). Our study sites are underlain by granodiorite bedrock (Bateman and Wones, 1972) and mantled by weakly developed soils comprising Entisols and Inceptisols (Bales et al., 2011). The main vegetation cover is Sierran mixed conifer comprising *Pinus ponderosa, Pinus lambertiana, Abies concolor* and *Libocedrus decurrens* (McCorkle et al., 2016).

Soil water and stream water pH ranges from 5.5 to 7. We estimate the soil production rate from the total denudation rate from cosmogenic nuclides which is ~220 t km^{-2} yr^{-1} (Dixon et al., 2009). This weathering regime is kinetically ~~limited and soils are only partially depleted in mineral nutrients. In contrast, the dust input is minor at 1 to 10 t km^{-2} yr^{-1} (Mahowald et al., 2005) and can be neglected in this study.~~ limited and soils are only partially depleted in mineral nutrients. Concerning dust inputs, Aciego et al. (2017) recently suggested that P supply by dust deposition outpaces local bedrock-derived P supply at the SSCZO for ecosystems developed over P-poor bedrock. However, estimates of the influence of dust inputs on nutrient dynamics are minor compared to the total denudation rate at our sites, with inputs of 3 to 36 t km^{-2} yr^{-1} (Aciego et al., 2017). Importantly, the total denudation rate of 220 t km^{-2} yr^{-1} (Dixon et al., 2009) measured at this site is higher than the range of denudation rates of 103 - 175 t km^{-2} yr^{-1} used in Aciego et al. (2017), and the P bedrock concentrations are higher in the Providence catchments studied here. We excluded the catchments comprising P-poor bedrock at site D102 ("Duff Creek"). The ratio of elemental dust deposition to the local, bedrock-derived elemental supply flux (referred to as RP^{X} in the following) amounts to less than 4 % for K, Ca and Mg and to 5.3 % for P at our sites and agrees with data shown in Aciego et al. (2017) for the P-rich bedrock. Therefore, the atmospheric supply flux of mineral nutrients can be considered to be insignificant relative to the local long-term supply fluxes from weathering.~~The main vegetation cover is Sierran mixed conifer comprising *Pinus ponderosa*, *Pinus lambertiana*, *Abies concolor* and *Libocedrus decurrens* (McCorkle et al., 2016).~~

Formatiert: Schriftart: Times New Roman, 10 Pt., Nicht Fett

2.2 Analytical methods

The chemical composition of soil, saprolite and rock samples were analysed by X-ray fluorescence spectrometry (XRF, Panalytical Axios Advanced) on fused tablets at GFZ Potsdam or by Acme Labs, Canada, with uncertainties better than 10 % relative. Additional concentration data was compiled from Hahm et al. (2014) and Riebe and Granger (2013). Element concentrations in plant material were analysed by an Inductively Coupled Plasma Optical Emission Spectrometer (ICP-OES, Varian 720ES) with uncertainties better than 15 %, after complete dissolution in HNO_3/H_2O_2 in PFA vials on a hotplate or using a microwave digestion system as successfully applied in previous Mg isotope studies (e.g~~.,~~. Bolou-Bi et al., 2012). Dissolved element concentrations in water samples were analysed by ICP-OES following the procedure described in Schuessler et al. (2016), Inductively Coupled Plasma Quadrupole Mass Spectrometry (Q-ICP-MS, Thermo iCAP-Q), and ion chromatography (Thermo Dionex DX-120) with uncertainties better than 10 %, respectively. All data of samples and reference materials (for assessment of analytical uncertainties) are reported in Tables S1~~ to S3.~~, S2 and S3a - S3c.

2.3 Mg isotope analyses by MC-ICP-MS

Mg stable isotope analyses have been performed at GFZ Potsdam, Helmholtz Laboratory for the Geochemistry of the Earth Surface (HELGES). Samples and reference materials were digested in PFA vials using ultra-pure acid mixtures (HF, HCl, HNO_3, H_2O_2). The exchangeable Mg fraction of soil and saprolite samples was obtained by a 1 M NH_4OAc extraction (Arunachalam et al., 1996). This procedure was specifically tested for Mg isotope measurements (Bolou-Bi et al., 2012). After extraction, the residual solids were analysed after HF/HNO_3 total digestion. Before isotope analysis, Mg was separated from other matrix elements by column chromatography (AG50W-X12 resin) following the procedure described in Pogge von Strandmann et al. (2011). Matrix elements were eluted with 1 M HNO_3, and then Mg was collected by elution with 2 M HNO_3. Purity of the Mg solutions as well as Mg yields were verified by analyses of final Mg-containing solutions using ICP-OES or Q-ICP-MS. Mg isotope ratios were measured with a Multi Collector Inductively Coupled Plasma Mass Spectrometer (MC-ICP-MS, Thermo Neptune). All sample solutions were diluted in 0.3 M HNO_3, where the samples Mg concentration was closely matched to those of the bracketing standard DSM-3. Results are expressed as the ‰ difference of the Mg isotope ratio of the sample relative to the DSM-3 isotope reference material (Galy et al~~.~~., 2003) using the delta notation: $\delta^{26}Mg = [(^{26}Mg/^{24}Mg)_{sample}/(^{26}Mg/^{24}Mg)_{DSM3} - 1] \times 1000$. The uncertainty is estimated to be ±0.10 ‰ (2SD) for $\delta^{26}Mg$, respectively, based on repeat measurements on reference materials (Tables S1~~ to S3~~, S2, S3c).

2.4 Mg isotope analyses by fsLA-MC-ICP-MS

The micro-scale Mg isotope composition of individual minerals (amphibole and biotite) was determined on a thin section of sample BP-0c (from the bedrock-saprolite interface) by UV femtosecond laser ablation coupled to a Thermo Neptune MC-

ICP-MS (~~fs LA~~fsLA-MC-ICP-MS, *Fem2*) at GFZ Potsdam. Instrumentation, data acquisition and evaluation procedures are described in detail in Schuessler and von Blanckenburg (2014). Laser ablation was performed on individual mineral grains with a spatial resolution of less than 200 x 200 µm surface area with less than 10 µm crater depth. The laser beam with a diameter of about 25 µm was scanned across the mineral surface to adapt to the irregular shape of the grains and cracks with repetition rates between 13 to 20 Hz. The high mass resolution mode of the MC-ICP-MS was used for Mg isotope ratio measurements. With high mass resolution, isobaric interferences ($^{52}Cr^{2+}$ on $^{26}Mg^{+}$, $^{50}Ti^{2+}$ and $^{50}Cr^{2+}$ on $^{25}Mg^{+}$, or $^{48}Ca^{2+}$ and $^{48}Ti^{2+}$ on $^{24}Mg^{+}$) can be resolved from Mg isotopes (Meng-Ning et al., 2016; Oeser et al., 2014). Mass bias correction was performed using the komatiite glass GOR132-G as bracketing standard. Using a $\delta^{26}Mg$ value for GOR132-G of -0.17 ‰ relative to DSM-3 (Oeser et al., 2014), we converted results to δ-values relative to DSM-3. Based on our current experience, we conservatively estimate the uncertainty of the fsLA-MC-ICP-MS method for Mg isotope ratios to be better than ±0.25 ‰ (2SD) for $\delta^{26}Mg$. Repeat measurements on reference material BHVO-2G (basaltic glass) (average $\delta^{26}Mg = -0.07 \pm 0.18$ ‰, 2SD, n=18) agree within uncertainties to published values ~~(Fig. 1)~~(Fig. 1) for this reference material (−0.20 ± 0.07 ‰, Meng-Ning et al., 2016). Results of biotite and amphibole analyses are presented in ~~Fig. 1.~~Fig. 1. Photomicrographs ~~(Fig. 2)~~(Fig. 2) show representative analysis locations in amphibole and biotite before and after laser ablation.

3 Results

3.1 Mg isotopic composition of ecosystem compartments

The Mg isotopic composition ~~(Fig. 3,~~(Fig. 3, Tables S1~~ to S3~~, S2, S3c) of mean bulk rock ($\delta^{26}Mg_{rock} = -0.22$ ‰ ± 0.10 ‰, 2SD) is identical within uncertainties to mean bulk regolith ($\delta^{26}Mg_{reg} = -0.15$ ‰ ± 0.13 ‰, 2SD) and mean suspended sediment ($\delta^{26}Mg_{susp.sed} = -0.30$ ‰ ± 0.16 ‰, 2SD). Results of analyses on biotite and amphibole on a thin section of rock sample BP-0c indicate that Mg-bearing minerals in the bedrock are not distinguishable in $\delta^{26}Mg$ within analytical uncertainties and are also identical to the bulk bedrock value of sample BP-0c ~~(Fig. 1).~~(Fig. 1). $\delta^{26}Mg$ in wood from growing trees ranges from -0.21 to +0.16 ‰, and $\delta^{26}Mg$ in growing foliage is lower than wood, i.e., -0.72 to -0.10 ‰. $\delta^{26}Mg$ of foliage, twigs, bark, and needles sampled from the forest floor and from the gauged creek sediment pond are within the range found in living foliage~~.~~ (Fig. 3). The intra-plant differences are consistent with previous studies that have shown that during translocation ^{24}Mg is preferred by the foliage whereas ^{26}Mg is preferred by wood (Black et al., 2008; Bolou-Bi et al., 2012). Despite the low $\delta^{26}Mg$ in foliage, bulk tree ($\delta^{26}Mg_{tree} \approx -0.07$ ‰, see mass balance calculation in Appendix A) is not distinguishable from bulk soil and rock. Only Mg in creek water ($\delta^{26}Mg_{diss} = -0.76$ ‰ ± 0.11 ‰, 2SD) and exchangeable Mg from soil and saprolite ($\delta^{26}Mg_{exch} = -0.68$ ‰ ± 0.36‰, 2SD) differ from the solid compartments. $\delta^{26}Mg_{diss}$ is remarkably constant throughout one hydrological water year and is in the range of global rivers draining silicate catchments (Tipper et al., 2012 and references therein). Results of element concentration measurements in rock, saprolite, soil, vegetation, water, and sediment samples are reported together with field measurement data (pH, temperature, conductivity, discharge, alkalinity) in T~~t~~ables S1~~ to S3~~, S2, S3a - S3c.

4 Discussion

4.1 Mg isotope fractionation by clay formation

Neoformation of Mg-clays is a mechanism that preferentially removes ^{26}Mg from soil solution and enriches this heavy isotope in Mg-clays such as smectite, illite or vermiculite (Wimpenny et al., 2014; Ryu et al., 2016). Clay formation is thus a potential cause for the low $\delta^{26}Mg_{diss}$ observed in the Providence Creek streams. ~~However~~Three independent lines of evidence all suggest that this effect is insignificant at our site. First, Mg-clay abundances are beneath the 5 % detection limit of XRD analysis~~ and~~. Second, their absence was confirmed by thermodynamic modelling (PhreeqC). ~~We~~Third, we use an isotope mass balance based on bulk soil Mg isotope composition to evaluate whether the low δ^{26}Mg of dissolved Mg could~~, however,~~ nevertheless be due to preferential incorporation of ^{26}Mg into small amounts of Mg-clay.~~ The abundance of Mg-clay was beneath the limit of detection of XRD.~~ In an isotope mass balance (Eq. (1)) we assign $\delta^{26}Mg_{bulk\ soil}$ the value of the isotopically heaviest soil sample (-0.05 ‰, see Table ~~S3~~S3c), which has the potential to be most affected by Mg-clay formation; and for primary minerals $\delta^{26}Mg_{prim}$ we use the rock mean $\delta^{26}Mg_{rock}$ (-0.22 ‰, Table ~~S3~~S3c).

$$\delta^{26}Mg_{bulk\ soil} = \delta^{26}Mg_{sec} \cdot f_{sec}^{Mg} + \delta^{26}Mg_{prim} \cdot \left(1 - f_{sec}^{Mg}\right)$$

~~(1)~~.

(1)

We first solve Eq. (1) for $\delta^{26}Mg_{sec}$ with f_{sec}^{Mg} ~~of 4 % which corresponds to~~ , the fraction of Mg ~~derived from~~ borne by secondary minerals is estimated to be 4 % which is contained in an upper possible limit of 5 % Mg-clay (XRD detection limit) ~~and~~relative to 20 % amphibole/biotite in bulk soil (Appendix B). Soil Mg isotopes can only be explained if δ^{26}Mg in secondary minerals ($\delta^{26}Mg_{sec}$) ≥ 4 ~~‰, which is unlikely (Wimpenny et al., 2014).~~‰. To our knowledge, such high clay δ^{26}Mg values have never been reported to date (Wimpenny et al., 2014). These clay δ^{26}Mg values would require that Mg-clays precipitate from dissolved Mg having a δ^{26}Mg of ~3.5 ‰, which has never been observed either (Tipper et al., 2012 and references therein). Second, we solve Eq. (1) for f_{sec}^{Mg} by using the maximum published $\delta^{26}Mg_{sec}$ of 0.5 ‰ (Ryu et al., 2016 and references therein). This clay value is also consistent with a Rayleigh-type mass balance constrained by the δ^{26}Mg of measured stream water and bulk rock as source Mg using $\alpha_{solid\text{-}solution} = 1.00054$ (Ryu et al., 2016). In this case the bulk soil Mg-clay content were 30 %, far in excess of our XRD analyses (Appendix B).

Therefore, incorporation of Mg into clays does not drive the low δ^{26}Mg of dissolved Mg~~ cannot be attributed to incorporation into clays.~~. The remaining process that depletes soil water in ^{26}Mg is the preferential uptake of ^{26}Mg by plants (Black et al., 2008; Bolou-Bi et al., 2012) associated with an isotope fractionation factor between plant Mg and dissolved Mg in the soil solution, expressed as $\Delta^{26}Mg_{plant\text{-}diss}$.

4.2 Mg tree uptake fractions from an isotope mass balance

We quantify the fraction of Mg uptake by higher plants (f^{Mg}_{uptake}) by ~~a closed system mass balance by Eq. (2) (Black et al., 2008; Johnson et al., 2004):~~an equation frequently used in stable isotope geochemistry (e.g. Black et al., 2008; Johnson et al., 2004) to calculate the partitioning of an element between two distinct compartments (Eq. (2)). This equation is derived from a simple "closed system" mass balance model, where the element can freely exchange between the two compartments (which are in turn isolated from any other compartment), and fractionate isotopically between these compartments. $\Delta^{26}Mg_{plant-diss}$ is the isotope fractionation factor between Mg in plants and dissolved Mg in soil water.

$$f^{Mg}_{uptake} = \frac{\delta^{26}Mg_{rock}-\delta^{26}Mg_{diss}}{\Delta^{26}Mg_{plant-diss}}.$$ ~~(2)~~

(2)

In Eq. (2) we use the isotopic difference between the "initial" $\delta^{26}Mg_{diss}$, and $\delta^{26}Mg_{diss}$ that has been modified from the initial soil solution by Mg uptake into plants. Since we do not know the initial $\delta^{26}Mg_{diss}$ we use $\delta^{26}Mg_{rock}$ as a proxy for this weathering solution, assuming congruent rock dissolution (Bouchez et al., 2013). It can be excluded that differences in primary mineral $\delta^{26}Mg$ lead to preferential release of specific $\delta^{26}Mg$, based on fs-laser ablation data of biotite and amphibole, the main Mg carriers, which are similar to $\delta^{26}Mg$ of bulk bedrock (Sect. 2.4 and ~~Fig. 1).~~Fig. 1). The f^{Mg}_{uptake} calculated here presents a minimum estimate ("net") of the total uptake fraction, as it does not include a fraction of Mg that is potentially recycled back into solution after uptake through Mg release from plant litter. We note that f^{Mg}_{uptake} calculated by Eq. (2) is mathematically equivalent to the results of the steady state flow-through reactor model of Bouchez et al. (2013) (see below), but here f^{Mg}_{uptake} reflects an instantaneous mass balance and does not depend on a steady state of fluxes, but applies only to an idealised closed system where plants exchange Mg with regolith water.

We can also describe both uptake and removal of Mg by a flow-through reactor isotope model (Bouchez et al., 2013~~).~~), where the isotope ratios are modeled as a function of elemental fluxes. Combining Eq. 3c, Eq. 3d and Eq. 5e from Bouchez et al. (2013) and assuming that no Mg is incorporated into secondary minerals leads to ~~Eq~~Eqs. (3) and (4):

$$\frac{\delta^{26}Mg_{rock}-\delta^{26}Mg_{diss}}{\Delta^{26}Mg_{plant-diss}} = \frac{U^{Mg}-S^{Mg}_{org}}{S^{Mg}_{rock}+S^{Mg}_{prim}}.$$ (3)~~$=\frac{E^{Mg}_{org}}{S^{Mg}_{rock}+S^{Mg}_{prim}}$.~~

~~(3)~~

$$\frac{\delta^{26}Mg_{rock}-\delta^{26}Mg_{diss}}{\Delta^{26}Mg_{plant-diss}} = \frac{E^{Mg}_{org}}{S^{Mg}_{rock}+S^{Mg}_{prim}}.$$ (4)

The denominator in ~~Eq.~~the right-hand terms of Eqs. (3) and (4) represents the sum of the Mg supply fluxes from rock dissolution (S^{Mg}_{rock}) at the weathering front and from primary minerals remaining in the regolith (S^{Mg}_{prim}). ~~The~~In Eq. (3) the flux term U^{Mg} quantifies the Mg uptake flux by trees. S^{Mg}_{org} represents the flux of Mg from ~~re-mineralisation~~leaching of plant litter that is either recycled back into the plants, or discharged into the river. ~~Note~~The difference U^{Mg}- S^{Mg}_{org} is therefore the net Mg accumulation in the "organic" compartment, combining living biomass and plant litter. The use of Eq. (3) does not rely on any steady-state assumption regarding this organic compartment, meaning that the ~~left-hand and middle term of Eq. (3) is identical~~equation applies even if this pool grows, for example during forest growth after deforestation or climate change. If the organic Mg pool is at steady state, the difference U^{Mg}- S^{Mg}_{org} is equal to ~~the determination of the relative Mg uptake flux f^{Mg}_{uptake}~~E^{Mg}_{org}~~,~~ where E^{Mg}_{org} refers to the particulate organic Mg export by ~~a closed system mass balance~~erosion (Eq.~~ (2~~ (4)). The isotope ratios are thus set by the Mg uptake flux by trees relative to the solubilisation flux of Mg by chemical weathering. ~~The combination of the middle term in Eq. (3) with its isotopic expression in the left-hand term does not require fluxes that are steady with time and is applicable to the transient growth of biomass. The equation can be expanded into the right-hand steady state term by assuming that in a steadily eroding weathering regime over the time scale of soil formation Mg initially released by weathering is also removed from the ecosystem by a) the dissolved export, and b) particulate export in plant litter including CWD (E^{Mg}_{org}).~~Note that the left-hands term of Eqs. (3) and (4) is identical to the one used for the determination of the relative Mg uptake flux f^{Mg}_{uptake} by a closed system mass balance (Eq. (2)). As the formation of Mg-clays or the dissolution of carbonates do not affect Mg fluxes at our study sites (Sect. ~~3.2~~4.1, Bateman and Wones, 1972), an isotope difference between rock and dissolved Mg only emerges if a substantial fraction of isotopically fractionated Mg accumulates in wood of a regrowing forest after clear cutting, or is exported in plant litter or CWD.

To estimate a range for f^{Mg}_{uptake} (Eq. (2)), or, at steady state, ~~E^{Mg}~~ E^{Mg}_{org} (Eq. (3)), we applied Eq. (2) and Eq. (~~3~~4) to all individual Providence Creek water samples by using a minimum and maximum $\Delta^{26}Mg_{plant\text{-}diss}$ of 0.50 ‰ (Opfergelt et al., 2014) and 0.68 ‰ (Black et al., 2008), respectively, and considered the analytical uncertainty on $\delta^{26}Mg$ of 0.10 ‰ (2SD). The difference of 0.~~5 ‰~~50 ‰, we found between $\delta^{26}Mg_{diss}$ and $\delta^{26}Mg_{rock}$, shows that 50 % to 100 % of the Mg initially released by chemical weathering is taken up by trees, and accumulates in growing forest biomass, or is eventually eroded in plant litter and CWD. Consequently, because of the high fraction of Mg uptake, the mean weighted $\delta^{26}Mg_{tree}$ is identical to bulk rock ~~(Ref462055945 * MERGEFORMAT Fig. 3)~~(Fig. 3). Therefore, at Providence Creek Mg is strongly bio-utilised.

Mg isotopes are unevenly partitioned into the different tree compartments comprising roots, trunk wood and non-woody foliage. Even though bulk tree $\delta^{26}Mg$ is higher than $\delta^{26}Mg_{diss}$, its composition is close to that of the parent rock and soil (Fig. 3). The reason is that during tree growth, the Mg taken up is partitioned into a high~~-~~$\delta^{26}Mg$ compartment in woody plant matter, and a low-$\delta^{26}Mg$ compartment in leaves and needles. However, to explain the deficit in ^{26}Mg in dissolved stream Mg, a high~~-~~ $\delta^{26}Mg$ compartment has to accumulate in wood, or be eroded~~, which could be located in the~~ as plant debris ~~contained in~~ present on the forest floor ~~material~~ and then exported as river ~~particulate matter~~particulates. We analysed $\delta^{26}Mg$ of foliage, twigs and bark sampled from the forest floor and a sediment pond containing the erosion products of the ecosystem. Forest floor and sediment pond needles (Fig. 3, Table S2) are isotopically light as expected, given that needles become isotopically lighter as they age (Bolou-Bi et al., 2012). ~~Twigs (~~Fine twigs (Fig. 3, Table S2) are isotopically light too. This finding is in contrast with the isotope composition we found in living wood ~~(Fig. 3),~~(Fig.3), and isotopically heavy Mg published for wood (Black et al., 2008; Bolou-Bi et al., 2012). The low δ^{26}Mg of the fine twigs (diameter ~3 mm) is explained by their Mg isotopic composition being dominated by bark for which we also found low δ^{26}Mg~~,~~ (Fig. 3), consistent with Chapela Lara et al. (~~2016~~2017). Regardless, the compartment containing the required high-δ^{26}Mg fraction is not contained in ~~these samples.~~

fine plant matter present on the forest floor, making CWD a more likely vector of export for this high-δ^{26}Mg component. However, the high-δ^{26}Mg fraction is found in the wood of tree trunks (Fig. 3, Table S2). ~~We interpret this observation to mean that the high δ^{26}Mg fraction contained in solid plant debris is exported only to a minor fraction contained in eroded foliage, and to a large fraction contained in exported tree trunks.~~ Our isotope mass balance allows for two ~~export mechanisms~~explanations: transient growth of tree biomass following logging and mechanical removal of tree trunks (~~middle term in~~ Eq. (3)); or natural erosion of coarse woody debris (CWD), at steady state with its uptake, with only minor leaching of Mg (~~right-hand term in~~ Eq. (~~3~~4)). We return to discussing these mechanisms in Sect. ~~3.9~~4.8.

4.3 Mg weathering fluxes from an isotope mass balance

The fact that Mg is highly bio-utilised and ~~eventually~~most likely eroded as CWD dictates that the dissolved Mg export ~~fraction~~flux is low~~.~~ relative to other Mg fluxes in the ecosystem. We use the isotope mass balance model (Bouchez et al., 2013) to calculate the normalised dissolved Mg export ~~fraction~~flux (~~w_{iso}^{Mg})~~$w_{isotope}^{Mg}$~~,~~ Tab. 1) by Eq. (~~4~~5) and report the data in Table S4b:

$$\cancel{w_{iso}^{Mg}}\, w_{isotope}^{Mg} = \frac{\delta_{topsoil}^{Mg}-\delta_{rock}^{Mg}}{\delta_{topsoil}^{Mg}-\delta_{diss}^{Mg}}. \qquad \cancel{(4)}$$

(5)

This fraction reflects the Mg solute export from the whole system relative to the total Mg export of solutes and particulates ~~in~~as primary and secondary minerals plus ~~plant litter.~~organic material. Estimating ~~w_{iso}^{Mg}~~$w_{isotope}^{Mg}$ does not depend on knowing isotope fractionation factors~~.~~, but it assumes a steady state of fluxes.

We use the mean δ^{26}Mg of unweathered rock, spatial- and time-integrated creek water of the individual Providence Creek sites (P301, P303, P304), and mean bulk ~~topsoil~~ soil and saprolite from the P301 soil profile and the soil-saprolite Balsam Profile ~~(Fig. 3). Topsoil~~(Fig. 3). The mean δ^{26}Mg of bulk soil and saprolite was chosen as soil and saprolite samples vary insignificantly in their δ^{26}Mg (similar results would be obtained if we had used the topsoil signature only, where topsoil is the compartment that is undergoing erosion at our sites). We consider the isotope composition of this soil-saprolite average to be more representative ~~of~~for exported particulate matter ~~compared to creek~~than samples from sediment ponds, because hydrodynamic sorting in the creek channel does not allow representative sampling of sediment~~. Because~~ from these ponds, where coarse, dense particles are enriched. δ^{26}Mg of topsoil, saprolite, and bulk rock are identical within their analytical uncertainties~~ we calculate ~~. Therefore only a potential upper boundary of the ~~possible Mg~~ relative Mg weathering flux ~~w_{iso}^{Mg}~~$w_{isotope}^{Mg}$ can be estimated by propagating the analytical uncertainties as in Bouchez et al. ~~(2013). We determined w_{iso}^{Mg} only for Mg and did not attempt isotope analyses of other bio-elements. The analysis of stable potassium (K) isotopes is not yet routine due to analytical limitations (Wang and Jackobsen, 2016). Isotopic fractionation of calcium (Ca) during uptake by plants does not appear to sufficiently shift the isotopic composition of water from that of its source rock as indicated by global compilations (Bouchez et al., 2013; Fantle and Tipper, 2014). Phosphorus (P) has only one stable isotope, and silicon (Si) isotopes fractionate by neoformation of secondary minerals or adsorption onto e.g. goethite (both are present in minor amounts at Providence Creek as determined by thermodynamic modelling (PhreeqC)) into the same direction as Si uptake by plants (Opfergelt and Delmelle, 2012~~(2013).

Our results show that according to Eq. (~~4~~5) only ~~14~~11 ± 13 % of Mg is exported from the weathering zone in the dissolved form ~~(Fig. 4).~~(Fig. 5). Therefore, the complementary ~~86~~89 % of Mg is exported predominantly in ~~silicate~~primary minerals and in a substantial proportion of CWD.

4.4 Elemental dissolved river fluxes

Next, we calculate an independent estimate of the relative dissolved Mg river flux (~~w_{diss}^{Mg}~~w_{river}^{Mg}) that allows comparison with the isotope-based dissolved Mg export (~~w_{iso}^{Mg}~~$w_{isotope}^{Mg}$). We also calculate the dissolved river flux ~~w_{diss}^{X}~~w_{river}^{X} for the ~~elements~~macronutrients (X) ~~Si,~~ K, Ca, P and ~~P.~~the plant beneficial element Si (hereafter we call these elements "bio-elements"). The absolute (non-normalised) dissolved annual river fluxes for these elements (~~W_{diss}^{X})~~W_{river}^{X}, Fig. 4, Tab. 1) are derived from Eq. (~~5~~6), which is the sum of the catchment area (A) normalised products of daily dissolved creek water concentrations ($[X]_{\cancel{diss}river_i}$) and daily discharge ($Q_i$) of one hydrological water year:

~~$$W_{diss}^{X} = \sum_{i=1}^{365} \frac{[X]_{diss_i} \cdot Q_i}{A} \qquad (5)$$~~

$$W_{river}^{X} = \sum_{i=1}^{365} \frac{[X]_{river_i} \cdot Q_i}{A} \qquad (6)$$

Since we lack daily resolution $[X]_{\cancel{diss}river}$ data and our sampling years (~~2004-~~2010-2014) differ from the hydrological water years (2004-2010~~-2014~~) for which daily discharge is available (http://criticalzone.org/sierra/data), we use the $[X]_{river}$-Q linear regression to determine daily ~~$[X]_{diss_i}$.~~$[X]_{river_i}$. We calculate mean discharge values from 15 days before to 15 days after each of our seven $[X]_{\cancel{diss}river}$ data points for all hydrological water years 2004 to 2010 and calculate annual ~~W_{diss}^{X}~~W_{river}^{X} for the individual hydrological water years 2004-2010 by applying Eq. (~~5~~6). We calculate an average of all hydrological water years 2004 to 2010 to derive ~~W^X_{diss}~~W^X_{river} (Table S4a). For example, catchment average ~~W^{Mg}_{diss}~~W^{Mg}_{river} range from about ~~7700~~7,700 to 28,000 ~~t~~mol km^{-2} yr^{-1}.

To allow comparison between flux estimates of different elements, we normalise the measured fluxes ~~to the same metric. We use~~using the elemental regolith production rate (RP^X, Fig. 4, Tab. 1, Table S4a), which quantifies the total transfer of an element X from bedrock to regolith at the weathering front, partitioned into secondary minerals, solutes, and remaining primary minerals (Bouchez et al., 2013) by Eq. (~~6~~7):

$$RP^X = D \cdot [X]_{rock}$$

~~(6)~~ (7)

Here, we use the total denudation rate (D, Tab. 1) from cosmogenic *in situ* ^{10}Be concentration from Dixon et al. (2009). Using D of 220 t km^{-2} yr^{-1} for all catchments and $[Mg]_{rock}$ of 1.9 weight-%, ~~RP^{Mg}~~RP^{Mg} is about 175,000 mol km^{-2} yr^{-1}. The normalised dissolved river fluxes (~~w^X_{diss}~~w^X_{river}) are calculated by Eq. (~~7~~8) (Bouchez et al., 2013) and reported in Table S4b:

~~$w^X_{diss} = \frac{W^X_{diss}}{RP^X}$.~~ ~~(7)~~

~~w^{Mg}_{diss}~~$w^X_{river} = \frac{W^X_{river}}{RP^X}$. (8)

w^{Mg}_{river} amounts to 4-16 % ~~(Fig. 4)~~(Fig. 5) of Mg fluxes, and is similarly low as ~~w^{Mg}_{iso}~~$w^{Mg}_{isotope}$ of ca. ~~14 %, supporting~~11 %. Thus, in the ~~notion that a substantial fraction of dissolved~~absence of Mg-containing secondary minerals, Mg is ~~taken up~~exported predominantly in remaining primary minerals, or, after uptake by plants~~ and subsequently eroded as~~, in the form of CWD or remains in the wood of a growing forest.

4.5 Net elemental solubilisation fluxes in the weathering zone

To test the interpretation that a substantial fraction of Mg and other bio-elements (X) ~~are exported~~ initially solubilised from rock accumulate in wood (with or without subsequent export as plant litter and CWD), we compare the relative dissolved export fluxes of Mg ~~w^{Mg}_{diss}~~w^{Mg}_{river} and ~~w^{Mg}_{iso}~~$w^{Mg}_{isotope}$ to the normalised net solubilisation flux (~~w^{Mg}_{τ}~~$w^{Mg}_{regolith}$, Table S4b). The non-normalised net solubilisation flux (~~W^X_{τ})~~$W^X_{regolith}$, Fig. 4, Tab. 1) is determined by Eq. (~~8~~9) and reported in Table S4a:

~~W^X_{τ}~~$W^X_{regolith} =$ ~~D~~$RP^X \cdot (-\tau^X_{Zr})$ ~~$\cdot [X]_{rock}$.~~ ~~(8)~~.

(9)

~~W_{τ}^{X}~~$W_{\mathrm{regolith}}^{X}$ is defined as the flux of release of X from minerals undergoing weathering, minus the flux of incorporation of X into new minerals potentially formed during weathering reactions (e.g. clays~~).~~) over the regolith profile. ~~W_{τ}^{X}~~$W_{\mathrm{regolith}}^{X}$ thus quantifies the net release of X from the bedrock-regolith system. $W_{\mathrm{regolith}}^{X}$ is derived from the total denudation rate (D~~), loss fractions (τ^X), and~~, Tab. 1) bedrock concentrations ($[X]_{\mathrm{rock}}$) following Eq. (7), combined with elemental loss fractions (τ^X, Tab. 1). The loss fraction (τ^X) quantifies the depletion ($\tau < 0$) or enrichment ($\tau > 0$) of an element X relative to unweathered bedrock (Riebe et al., 2003). τ^X is determined by Eq. (~~9~~10):

$$\tau_{Zr}^{X} = \frac{[Zr]_{unweathered\ bedrock}}{[Zr]_{weathered\ regolith}} \cdot \frac{[X]_{weathered\ regolith}}{[X]_{unweathered\ bedrock}} - \cancel{1.} \qquad \cancel{(9)}1. \qquad (10)$$

Zr is used as the immobile element. In addition to the data set of this study, ~~additional~~published data (Hahm et al., 2014; Riebe and Granger, 2013) have been used to obtain the most representative bedrock concentrations and are reported with our data in Table ~~S3~~S3a - S3c.

The net solubilisation flux ~~W_{τ}^{X}~~$W_{\mathrm{regolith}}^{X}$ is determined by Eq. (~~8~~9) for each of the Providence Creek catchments and ranges from 41,000 to 75,000 ~~t~~mol km^{-2} yr^{-1} for Mg. Since τ^X is relatively uniform across the sampled soil-saprolite profile ~~(Fig. 6)~~(Fig. 7) mean τ^X-values based on soil and saprolite data from Hahm et al. (2014) and Riebe and Granger (2013) (Table S3) have been used. Only τ^P is strongly depth-dependent ~~(Fig. 6).~~(Fig. 7). Hence ~~the values~~we used ~~in this study are~~the most negative τ^P from the ~~mineral topsoil at 13-26 cm depth.~~dataset from Hahm et al. (2014) and Riebe and Granger (2013) (Table S3). The normalised net solubilisation flux (~~w_{τ}^{X}~~$w_{\mathrm{regolith}}^{X}$) is determined by Eq. ~~(10):~~(11). The comparison to equations (7) and (9) shows that $w_{\mathrm{regolith}}^{X}$ is actually equal to $-\tau_{\mathrm{Zr}}^{X}$:

$$\cancel{w_{\tau}^{X} = \frac{W_{\tau}^{X}}{RP^{X}}.} \qquad \cancel{(10)}$$

~~w_{τ}^{X} is equal to $-\tau_{Zr}^{X}$ and the regolith production rate of element X (RP^X) at depth is equal to the total denudation rate of element X.~~

$$\cancel{w_{\tau}^{Mg}} w_{regolith}^{X} = \frac{W_{regolith}^{X}}{RP^{X}} = -\tau_{\mathrm{Zr}}^{X}. \qquad (11)$$

$w_{\mathrm{regolith}}^{\mathrm{Mg}}$ ~~is much higher than $w_{\mathrm{iso}}^{\mathrm{Mg}}$ and $w_{\mathrm{diss}}^{\mathrm{Mg}}$ and~~ amounts to ~40 % ~~(Fig. 4),~~(Fig. 5), meaning that in the regolith 40 % of the Mg supplied from rock is transferred into the dissolved form ~~in regolith~~ and is made available for plant uptake. ~~The results of~~ Because $w_{\mathrm{regolith}}^{\mathrm{Mg}}$ is much higher than $w_{\mathrm{isotope}}^{\mathrm{Mg}}$ and $w_{\mathrm{river}}^{\mathrm{Mg}}$ (Sect. ~~3.3 show~~4.2), this calculation shows that a substantial fraction of Mg once released by chemical weathering is taken up ~~by plant and subsequently exported in Mg-containing CWD~~into the biomass without subsequent redissolution.

4.6 Dissolved export ~~fractions~~ efficiency

To confirm that Mg is not the only element that is strongly bio-utilised, we compared the dissolved river flux (~~W^X_{diss}~~W^X_{river}) with the net solubilisation flux (~~W^X_{τ}~~$W^X_{regolith}$) by its ratio ~~W^X_{diss}~~W^X_{river}/~~W^X_{τ}~~$W^X_{regolith}$ for ~~macronutrients (X) like K, Ca, P and~~ the ~~plant-beneficial element Si. This approach requires knowing the denudation rate D (Eq. (8)) from cosmogenic nuclides, and the discharge Q (Eq. (5)) from long-lasting gauging programs. Using directly the ratio W^X_{diss}/W^X_{τ} would be associated with large uncertainties because both methods integrate over entirely different time scales. To obtain a metric that is independent of D and Q, we normalised the fluxes W^X_{diss} and W^X_{τ} over their respective Na fluxes (Eq. (11)) and rearrange to the right-hand term of Eq. (11):~~

~~$DEF^X = \frac{\frac{W^X_{diss}}{W^{Na}_{diss}}}{\frac{W^X_{\tau}}{W^{Na}_{\tau}}} = \frac{\left(\frac{[X]_{diss}}{[Na]_{diss}}\right)/\left(\frac{[X]_{rock}}{[Na]_{rock}}\right)}{\frac{(\tau^X_{Zr})}{(\tau^{Na}_{Zr})}}$. (11)~~

~~Na is the element of choice since it behaves conservatively, meaning Na is neither incorporated into secondary minerals nor taken up as a nutrient by plants. We call the Na-normalised ratio between W^X_{diss} and W^X_{τ} the dissolved export fraction (DEF^X, Eq. (11), Fig. 5). The DEF^X~~other bio-elements (K, Ca, P, Si). Because this ratio quantifies the dissolved riverine loss of X from the ecosystem relative to its net release from the regolith~~. At steady state, the DEF^X~~ we call the ratio the “dissolved export efficiency” (DEE^X, Eq. (12), Fig. 6, Tab. 1):

$$DEE^X = \frac{W^X_{river}}{W^X_{regolith}}. \qquad (12)$$

If the DEE^X is larger than 1, input sources other than rock weathering are supplying X, such as atmospheric deposition (see Sect. 5.0). The DEE^X is less than 1 if some of the released element is partitioned into a plant uptake flux ~~and then~~during forest growth or is eroded as plant litter or CWD (including eroded phytoliths in the case of Si). ~~If the DEF^X is larger than 1, other inputs are needed to explain the X mass balance, such as atmospheric deposition, for example.~~

The ~~only case~~DEE^X can also differ from 1, because W^X_{river} and $W^X_{regolith}$ integrate over entirely different time scales. The inferred DEE^X (~ 0.40 for K, ~0.60 for Ca, ~0.30 for Mg, ~0.05 for P and ~0.10 for Si) of each nutritive element is less than 1 (Fig. 6) suggesting that some fractions of bio-elements once released by chemical weathering are bio-utilised and remain in ~~which~~ regrowing forest biomass after clear cutting or are eventually eroded as CWD. The DEE^X of the non-nutritive element Na is < 1 too and amounts to 0.68 (Table S4d). Thus, DEE^{Na} suggests that 32 % of Na, which has been released by chemical weathering, is missing in the dissolved river flux. This result is unexpected because Na behaves conservatively, meaning Na is neither incorporated into secondary minerals nor taken up as a nutrient by plants. Measured Na in pine tree wood amounts

Formatiert: Englisch (Vereinigtes Königreich)

Formatiert: Englisch (Vereinigtes Königreich) to 3 - 8 ppm (Table S2) and in shrub wood to ~40 ppm (Table S2). These low Na contents in plants translate into a plant uptake flux of about 2 % relative to the solubilisation flux, far lower than the ~1/3 of $W_{\mathrm{regolith}}^{\mathrm{Na}}$ estimated from DEE$^{\mathrm{Na}}$. This observation agrees well with the fact that Na is only a plant beneficial element in halophylic and C4/CAM plants (Marschner, 2011) and plays no significant nutritive role in pine trees representing the prevailing plant species at SSCZO. We argue that the supposed deficit in $W_{\mathrm{river}}^{\mathrm{X}}$ relative to $W_{\mathrm{regolith}}^{\mathrm{Na}}$ is a time scale effect as $W_{\mathrm{river}}^{\mathrm{X}}$ integrates over annual and $W_{\mathrm{regolith}}^{\mathrm{X}}$ over millennial time scales.

To obtain a metric that is independent of time scale effects, we normalised the fluxes $W_{\mathrm{river}}^{\mathrm{X}}$ and $W_{\mathrm{regolith}}^{\mathrm{X}}$ over their respective Na fluxes (Eq. (13)) and rearrange to the right-hand term of Eq. (13):

$$DEE_{Na}^{X} = \frac{\frac{W_{river}^{X}}{W_{river}^{Na}}}{\frac{W_{regolith}^{X}}{W_{regolith}^{Na}}} = \frac{\left(\frac{[X]_{river}}{[Na]_{river}}\right)/\left(\frac{[X]_{rock}}{[Na]_{rock}}\right)}{\frac{\left(\tau_{Zr}^{X}\right)}{\left(\tau_{Zr}^{Na}\right)}}. \qquad (13)$$

This approach has a fundamental benefit, as knowing the denudation rate D (Eq. (9)) from cosmogenic nuclides, and the discharge Q (Eq. (6)) from long-lasting gauging programs is not required. However, we note that the Na normalisation may ~~not fully remove time scale issues is~~also introduce bias into the DEE$_{\mathrm{Na}}^{\mathrm{X}}$. This might be the case, if, for example, changes in water flow during the development of the profile over a few thousand years result in ~~non-steady~~a change in the stoichiometry of rock dissolution. Such changes in the congruency in the dissolution of rock might result from changes in the dissolution of Na-bearing primary minerals relative to other primary minerals, or ~~if the~~from a changing rate of secondary mineral formation ~~changes~~ relative to Na-bearing primary ~~mineral decomposition.~~minerals. In that case the time-integrated denominator in Eq. (~~11~~13) does not reflect the present value.

The ~~DEF$^{\mathrm{X}}$~~DEE$_{\mathrm{Na}}^{\mathrm{X}}$ values obtained ~~(Fig. 5, Table S4d~~(Fig. 6, Table S4e) show that, of the elements solubilised from rock, ~80 % of Ca, ~60 % of K, ~50 % of Si, ~40 % of Mg, and ~~~25~~10 % of P appear in the streams dissolved load. The ~~DEF~~DEE$_{\mathrm{Na}}^{\mathrm{X}}$ for Mg is in excellent agreement with the 50-100 % of Mg bio-utilisation calculated independently by isotope mass balances (Eq. (2)). The high ~~DEF~~DEE$_{\mathrm{Na}}^{\mathrm{X}}$ for Ca ~~is due~~can be attributed to its high concentrations in rock combined with its high degree of solubilisation by chemical weathering that ~~result~~results in excess availability compared to the nutrient demand of trees. In contrast, the low ~~DEF~~DEE$_{\mathrm{Na}}^{\mathrm{X}}$ for P is most likely due to its high biological demand and low availability, resulting in high degree of plant uptake and subsequent export in plant litter and CWD.

Formatiert: Nicht Hochgestellt/ Tiefgestellt

4.7 Nutrient recycling factor

After uptake and return to the forest floor, nutrients are not directly discharged into the stream by litter dissolution, or eroded as plant litter or CWD. Rather, they are subject to recycling - defined here as uptake of nutrients ~~released from plant litter. Note that if nutrient uptake into plants equals nutrient return from plants, recycling does not change the stable isotope ratios~~

~~of the involved compartments (Bouchez et al., 2013). In addition, the fluxes calculated above are net fluxes that do not take recycling into account. However, the recycling rate~~that are made bio-available again after their release from plant litter. The recycling flux can be hypothesised to depend on the ratio of nutrient demand to availability. We thus tested the hypothesis that in our kinetically-limited setting, unlike in the supply-limited regime, intense nutrient recycling is not required as nutrient loss can be balanced by ~~new uptake~~supply from ~~regolith~~mineral dissolution in the regolith (Jobbagy and Jackson, 2001; Lucas, 2001). In other words, if nutrient supply from regolith ($W^X_{regolith}$) is high, ecosystem nutrition can be satisfied even if recycling is low (Lang et al., 2016). We quantified nutrient recycling as the number of passages an element X takes through the vegetation after its initial release from rock (quantified by the net solubilisation flux ~~W^X_t~~$W^X_{regolith}$). We note that the nutrient uptake-release loop is distinct and formally independent of other fluxes such as regolith production, weathering, and export fluxes calculated above (Fig. 4). We call ~~this~~the number of passages in the loop the elemental recycling factor (Rec^X, Fig. 4, Tab. 1). Rec^X is determined by Eq. (~~12~~14) and reported in Table S4e:

Formatiert: Nicht Hochgestellt/ Tiefgestellt

$$Rec^X = \cancel{\frac{L^X}{W^X_t}}\frac{L^X}{W^X_{regolith}}. \qquad \cancel{(12)}$$

(14)

~~Because the~~The nutrient uptake flux is the product of net biomass productivity and biomass nutrient concentration (U^X~~)~~, Fig. 4). Since U^X is difficult to determine, we use the sum of litter fluxes (L^X) comprising foliage litter fall ($L^X_{foliage}$, Table S4c), root litter (L^X_{root}, Table S4c) and trunk litter (L^X_{trunk}, Table S4c) instead, assuming balanced uptake and litter fall fluxes~~.~~ (for input parameters see Appendix C). L^{Mg} is 16,000, 10,000 to 20,000, and 28,000 ~~t~~mol km^{-2} yr^{-1} for foliage, stem, and root, respectively. L^X represents a minimum estimate for U^X and hence Rec^X is likely underestimated because we did not consider return of growth-limiting nutrients from foliage via phloem through roots back into soil during senescence and return of nutrients from throughfall or stem flow. ~~Since litter data for Providence Creek is not available we use total foliage litter fall fluxes of *Pinus ponderosa* from literature (Grady and Hart, 2006; Klemmedson et al., 1990; Law et al., 1999) and multiply them with the elemental foliage litter concentration of *Pinus ponderosa* (Klemmedson et al., 1990) except for Si for which we used data from Bartoli (1983) to determine $L^X_{foliage}$. To determine L^X_{root} we used root litter production data from Röderstein et al. (2005) and since roots were not sampled in this study we used Mg, Ca and K root concentrations from *Picea abies* (Bolou-Bi et al., 2012), the P root concentration from *Pinus sylvestris* (George et al., 1997) and the Si *Pinus ponderosa* needle concentration from this study as elemental needle and root concentrations are generally similar and due to the lack of Si root concentration for coniferous trees in the literature. To determine L^X_{trunk} we estimated the *Pinus ponderosa* minimum and maximum trunk wood biomass by using an logging calculator (www.burleyboys.com, for input parameters see Appendix C) and *Pinus ponderosa* Mg, Ca, K and Si wood concentrations from this study and P wood concentration from *Pinus contorta* (Pearson et al., 1987).~~

Formatiert: Schriftfarbe: Automatisch

~~At Providence Creek, we observe that~~With an average $\mathrm{Rec}^{\mathrm{P}}$ of 13, P is the only bio-element that is tightly recycled (Fig. 6) and becomes enriched ~~(Fig. 6) and tightly recycled~~ in topsoil ~~(Fig. 5). Although $\mathrm{Rec}^{\mathrm{K}}$ is only slightly above unity we infer that K becomes~~(Fig.7). Aciego et al. (2017) also compared the sum of dust and bedrock-derived P supply fluxes with nutrient uptake fluxes at SSCZO, obtaining an order of magnitude higher uptake than supply fluxes, and concluded too that P is recycled ~~since~~. With $\mathrm{Rec}^{\mathrm{K}}$ of ca. 4, K is also recycled. We note that $\mathrm{Rec}^{\mathrm{K}}$ is likely underestimated due to the lack of throughfall data which are generally highest for K compared to the other bio-elements (Boy and Wilcke, 2008). The $\mathrm{Rec}^{\mathrm{X}}$ for the ~~other bio-elements (Fig. 5) is low. The low $\mathrm{Rec}^{\mathrm{X}}$ for the bio-elements but P is~~macronutrients Ca and Mg is about unity (Fig. 6) and thus these nutrients are not recycled by uptake after release from litter. This means that uptake from regolith is their only source. The $\mathrm{Rec}^{\mathrm{Si}}$ of < 0.1 means that only a minor fraction of Si solubilised from rock is bio-utilised. The low $\mathrm{Rec}^{\mathrm{X}}$ values for all bio-essential elements except P are in agreement with our observation that after uptake the largest mass fraction of these bio-elements remain in wood or is disposed through export of plant litter and CWD. ~~If nutrient supply from regolith were low, $\mathrm{Rec}^{\mathrm{X}}$ would be~~Altogether, the overall high ~~to satisfy ecosystem nutrition (Lang et al., 2016). At Providence Creek we observe a direct export pathway~~$\mathrm{DEE}^{\mathrm{X}}_{\mathrm{Na}}$ (section 4.6) and low $\mathrm{Rec}^{\mathrm{x}}$ is consistent with the kinetically-limited weathering regime of Providence Creek~~. –~~ in which mineral nutrients are supplied in sufficient demand, the ecosystem is "acquiring" and thus the need for recycling is low (Lang et al., 2016).

Although $\mathrm{Rec}^{\mathrm{X}}$ and $\mathrm{DEE}^{\mathrm{X}}_{\mathrm{Na}}$ rely on $W^{\mathrm{X}}_{\mathrm{regolith}}$ we note that both metrics are independent from each other. This independency arises because ecologic stoichiometry enriches other mineral nutrients in plants than released from mineral dissolution kinetics. Thus an element X can become recycled (meaning uptake of nutrients released from plant litter) many times compared to this element's weathering flux $W^{\mathrm{X}}_{\mathrm{regolith}}$. This number of cycles as quantified by $\mathrm{Rec}^{\mathrm{X}}$ can vary between 0 and a large number. In contrast, $\mathrm{DEE}^{\mathrm{X}}_{\mathrm{Na}}$ quantifies the fraction of an element that is exported in the dissolved river load rather than being contained in plant debris, relative to the fraction of X that was initially solubilised by chemical weathering, and can vary between 0 and 1 unless atmospheric input results in $\mathrm{DEE}^{\mathrm{X}}_{\mathrm{Na}} > 1$.

4.8 ~~Export mechanisms~~ Accumulation of bio-elements during forest growth or export in coarse woody debris (CWD~~)~~)?

In the preceding sections, we have ~~shown that bio-utilisation and solid export of CWD is required to~~suggested two mechanisms that potentially explain the creek water being enriched in ^{24}Mg, and the deficit in the dissolved river export fraction indicated by the ~~$\mathrm{DEF}^{\mathrm{X}}$. Here we discuss two CWD export mechanisms:~~$\mathrm{DEE}^{\mathrm{X}}_{\mathrm{Na}}$: 1) bio-utilisation and accumulation of bio-elements in wood of a~~) logging~~ regrowing forest after clear cutting on centennial time scales; ~~and b)~~or 2) solid export of nutrients in CWD by natural erosion in pre-~~anthropogenic~~forest management times and over weathering (~~ky~~kyr) time scales. Concerning logging, indeed in the late 19th century *Pinus ponderosa* forests became nearly wholesale clear-cut (Graham and Jain, 2005~~).~~) and our study sites underwent continuous logging of some form up through the 1960s (Carolyn Hunsaker, personal communication).

These logging activities triggered the growth of today's forest at Providence Creek and might have shifted the ecosystem from some quasi-steady state - where elemental input fluxes equal elemental export fluxes, and where plant growth equals plant mortality - into an ecosystem being in a transient state characterised by the build-up of a pool of bio-elements (e.g. Sommer et al., 2013). Concerning natural erosion, trunk wood that is enriched in ^{26}Mg is not contained in the sediment pond we sampled. Yet it is continuously removed from the ecosystem by stochastic events, such as ~~landslides,~~ tree turnover after tree death (Roering et al., 2010), wind throw, or ~~frequent~~ wildfires - that are suppressed since the late 19th century - after which ash is fast eroded.

To estimate whether tree trunk growth satisfies the elemental and isotopic mass balance we estimated the budgets of bio-elements contained in *Pinus ponderosa* trunk wood (see Sect. ~~3.8~~4.7 and Appendix C). We find that the ~~uptake~~litter fall fluxes (L^X, Table S4c) ~~are~~ that we use to estimate uptake indeed ~~similar to~~are comparable with the deficit in the elemental dissolved export ~~fraction~~flux as indicated by ~~the DEF^X~~1-DEE^{X}_{Na} for Mg and Ca. Both the P and K trunk wood fluxes are higher than ~~predicted by~~the deficit in the ~~DEF^X~~elemental dissolved export flux. This effect arises for strongly recycled elements, because the uptake flux contains the fraction added by nutrient recycling from the forest floor. ~~However, the Si tree trunk budget is two orders of magnitudes lower than predicted by the DEF^{Si}. The reason is that for most tree species stem wood contains at least one order of magnitude lower Si concentrations than leaves (Cornelis et al. 2009). Thus, the low DEF of Si can be explained by Si export occurring in the bio-opal of phytoliths of which the dissolution half-life at the pH prevailing at Providence Creek amounts to a few 100 days (Fraysse et al., 2009).~~However, for Si Rec^X amounts to <0.1 whereas the fraction not accounted for by dissolved loss (1-DEE^{X}_{Na}) is 0.54. A possible reason is that pine needles can treble in Si concentrations concentrations as the needles age (Cornelis et al., 2009), and that Si is bio-utilised by shrubs whose leaves dispose phytoliths that is not accounted for in our budget. Thus the Si concentrations used in our calculations might be unrepresentative of those in aged leaf litter (Appendix C) and Rec^{Si} might be an underestimate. If true, the 1-DEE^{X}_{Na} of Si amounting to 50% is a better estimate for Si uptake.

Whether natural erosion of bio-elements by CWD is a feasible mechanism depends on whether the erosional time scale outcompetes the leaching time scale from CWD. Trunk wood decomposition fluxes have been quantified for *Fagus grandifolia*, *Acer saccharum* and *Betula alleghaniensis*. About 25-50 % of Ca, 30-70 % of P, 5-20 % of K, 20-40 % of Mg (Johnson et al~~.~~., 2014), and 25-60 % of Si (Clymans et al., 2016) remain in trunk wood after 16 years of decomposition. For comparison, after 2 years of *Pinus ponderosa* foliage litter decomposition ~90% of Ca, ~55 % of P, ~20 % of K, ~45 % of Mg (Klemmedson, 1992) remain in foliage litter. ~~Thus~~The dissolution half-life of the bio-opal in phytoliths at the pH prevailing at Providence Creek amounts to a few 100 days (Fraysse et al., 2009). Therefore, bio-element leaching (except Ca) from foliage outpaces bio-element leaching from wood. Hence, after tree death and after ~~litterfall~~litter fall (Si contained in phytoliths, and Ca likely contained in oxalates) erosional removal must occur within this decomposition time scales for CWD to be a feasible mechanism.

Formatiert: Schriftart: 11 Pt.

Given the lack of information on the pre-logging fluxes and isotope ratios at Providence Creek we have no means to assess whether the natural CWD erosion mechanism has been in operation~~.~~ and caused the deficit in dissolved elemental export rather than forest growth today. We can speculate, however, that one effect has replaced the ~~export by logging is~~other with similar ~~to~~impact on fluxes. This is because the natural erosion of mineral nutrients in tree trunks in the form of CWD ~~as both are~~is ultimately limited by tree growth too. One other study, using stable Sr isotopes in an unperturbed ecosystem in New Zealand, shows a similar partitioning of Sr between plants and the river dissolved ~~-~~flux (Andrews et al~~,~~., 2016). That data can be interpreted to imply natural erosion of Sr in plant litter and CWD. The same interpretation is possible for the data from the Shale Hills Critical Zone Observatory, where a similar deficit in heavy Mg isotopes was found in stream and soil water (Ma et al~~.~~., 2015). In that study the bio-cycling hypothesis was dismissed on the grounds of missing accumulation of Mg in the organic~~-~~-rich portions of the soil. The existence of a sub-micron pool enriched in ^{26}Mg was hypothesised instead. However, the Mg data ~~would~~at Shale Hills CZO is be compatible with the CWD export hypothesis too.

4.9 Nutrient uplift from the deep saprolite

~~Finally, we determine~~We determined the depth from which these nutrients are uplifted. A first indicator is the depth distribution of loss fractions τ^X (Brantley and Lebedeva, 2011) that allows for the identification of so-called biogenic profiles that are characteristically depleted at depth and become enriched in topsoil, because nutrients are uplifted from depth (Jobbagy and Jackson, 2001; Lucas, 2001~~).~~; Bullen and Chadwick, 2016). Whereas P depletion amounts to 85 % at 3 m depth and increases towards the surface indicating biogenic uplift of P, the loss fractions of Mg, K, and Si amount to 20 to 40 % and show uniform depletion along the entire depth of the weathering zone down to 7 m depth. The traditional view is that this loss is induced by mineral dissolution and removal by infiltrating water (Brantley and Lebedeva, 2011). We can use Mg isotopes to explore an alternative hypothesis: that these ~~nutrients~~bio-elements are taken up by tree roots or associated myc~~r~~orrhiza fungi (Jongmans et al., 1997; Landeweert et al., 2001; Lucas, 2001) at these deep levels. In the absence of Mg-clays and carbonates the isotopically light composition of the exchangeable fraction throughout the regolith ($\delta^{26}Mg_{exch}$, ~~ERGEFORMAT Fig. 3)~~Fig. 3) can only be caused by the preferential uptake of heavy Mg isotopes by trees. We can exclude that the development of such an isotopically light exchangeable Mg compartment throughout the regolith is due to fractionation during adsorption (Opfergelt et al., 2014) as the associated fractionation factor is close to 0 ‰ (Wimpenny et al., 2014). Also, Bullen and Chadwick (2016) have shown that isotopic fractionation during adsorption onto clay minerals is absent for other bivalent cations. We can also exclude that low $\delta^{26}Mg_{soil\ water}$ infiltrates to depth from the surface as this $\delta^{26}Mg_{soil\ water}$ ~~-~~would be masked by the high Mg solubilisation flux from primary minerals ~~(Fig. 4).~~at the considered depth (Fig. 5). Deep water uptake from down to ~~7~~6 m is supported by the rooting depth of *Pinus ponderosa* which can reach up to 24 m (Stone and Kalisz, 1991).

~~5~~5.0 Atmospheric depositional fluxes

$\mathrm{DEE}_{\mathrm{Na}}^{\mathrm{X}}$, $\mathrm{Rec}^{\mathrm{X}}$, and the possible enrichment of nutrients from the deep saprolite to shallow soil might all be affected by external dust deposition. Aciego et al. (2017) recently suggested that P supply by dust deposition outpaces local bedrock P supply at the SSCZO in P-poor bedrock. We have argued in section 2.1 that this observation does not hold for the P-rich bedrock at our sites, nor when applied to the other mineral nutrients when long-term RP^{X} and $\mathrm{W}_{\mathrm{regolith}}^{\mathrm{X}}$ are considered. Aciego et al. (2017) also compared dust P inputs to modern P export from sediment trapping, which averages erosion over the annual to decadal timescales of human observations. However, measurements of modern sediment fluxes in streams are known to systematically underestimate erosion rates (total denudation rate minus chemical weathering rate) due to the episodic nature of sediment transport (Kirchner et al., 2001; Schaller et al., 2001). In addition, P export also occurs as dissolved species, which needs to be taken into account when estimating bedrock-derived P supply using export fluxes. For example, at SSCZO both the total dissolved river export $\mathrm{W}_{\mathrm{river}}^{\mathrm{P}}$ and the total weathering flux $\mathrm{W}_{\mathrm{regolith}}^{\mathrm{P}}$ that is calculated from cosmogenic nuclides, chemical depletion of regolith and bedrock P concentration exceed the P erosion flux from sediment trapping by one to two orders of magnitude. Because at these sites at most 58% of regolith production are partitioned into a dissolved flux (Dixon et al., 2009), the high recent dissolved flux needs to be associated with a complementary erosion flux. That this is not the case provides further evidence that the erosion flux determined by sediment trapping is a serious underestimate. Therefore from comparing our results with those of Aciego et al. (2017) we suggest that while dust input of P might be of significance to the local ecosystem on low-P substrate at SSCZO, it is insignificant for P and the other nutritive elements at our P-rich sites in the Providence Creek catchments.

6 Implications

Formatiert: Zeilenabstand: 1.5 Zeilen

To date the possible acceleration of weathering by plants has only been inferred indirectly, by comparing the flux of watersheds of different vegetation cover over short time scales (Moulton et al., 2000). At Providence Creek a substantial fraction of bio-elements released by rock dissolution over typical weathering time scales (thousands of years) is directly utilised by the local forest trees - where nutrient uptake does not depend on the mechanism of export. Our data provide ~~the first direct observation of~~ new insight into the role of biota ~~plays~~ in contributing to weathering fluxes in a given ecosystem. The partitioning of Sr stable isotopes in a mountain catchment in New Zealand (Andrews et al., 2016) can be interpreted in the same way. It is essential to both metal isotope-based observations that the ~~bio-~~elements taken up by plants are directly exported ~~in CWD~~as particulate organic material. The low recycling factors observed support this notion of rapid nutrient uptake and disposal. Therefore, in this kinetically-limited setting, this mechanism provides a possible tight coupling between weathering up to ~~7~~6 m depth ~~is tightly coupled to~~ and nutrient utilisation and erosion. We do not know whether this deep nutrient uptake is actively driven by nutrient demand (Brantley et al., 2011; Landeweert et al., 2001; Lucas, 2001), or is coupled to deep water uptake during summer droughts. Regardless, either cause would deepen the weathering advance front and potentially facilitates the balance between erosion and weathering advance rate~~ (Brantley et al., 2011).~~.

Considering that 30 % of the Earth's surface is covered by forests (Bonan, 2008) the export of the bio-utilised ~~bio-~~elements in CWD and bio-opal might represent a more widespread phenomenon. Indeed, in active mountain belts the weathering intensity (total chemical weathering rate normalised by denudation rate) derived from river loads is far lower than that derived from regolith (Dixon and von Blanckenburg, 2012). We suggest that one possible explanation for this discrepancy is the nutrient uptake by biota and its subsequent erosion as bio-opal, leaf litter, and CWD in these predominantly kinetically-limited weathering regimes. In contrast, in lowland supply-limited regimes and floodplains the low bio-element concentrations in plant debris, the low particulate organic matter sediment yield (0.1-1 % of total sediment yield) (Galy et al., 2015, Hilton, 2017) and the low amorphous opal flux (0.6 % of total sediment yield) (Frings et al., 2016) results in nutrient export to occur predominantly in the dissolved form. The postulated fast weathering and rapid nutrient erosion coupling is significant only in geologically active mountains where CWD and bio-opal erosion is high (Galy et al., 2015; McCorkle et al., 2016), outpaces nutrient recycling, and might constitute a significant solid export flux of elements released by weathering and hence not accounted for in weathering flux estimates based on dissolved river loads.

~~6~~7 Conclusions

The Mg isotope composition of stream water in the Providence ~~creek~~Creek watershed, Southern Sierra Nevada, requires a compartment separation between isotopically light Mg dissolved in water and isotopically heavy Mg accumulated in wood of a regrowing forest after clear cutting, or exported in tree wood, without substantial re-mineralis~~z~~ation and re-utilisation. A steady state isotope mass balance supports the solid Mg export path in that the Mg export is dominated by particulates, and only a minor fraction of ~~~14~~ca. 11 % of Mg is exported as solutes. ~~Thus~~Using Mg isotopes to quantify uptake, we found that 50-100 % of Mg that is released from primary minerals is utilised by trees. This high Mg bio-utilisation is confirmed by a deficit apparent in the Na-normalised dissolved river Mg export flux when compared to the Na-normalised net Mg solubilisation flux. The deficit of dissolved Mg (1-DEE$^{Mg}_{Na}$), exported by creeks, amounts to 60 %, meaning that 60 % of Mg is bio-utilised. We find similar deficits (1-DEE$^{X}_{Na}$) amounting to ~40 % for K, ~20 % for Ca, ~50 % for Si and ~~~75~~90 % for P. These three lines of evidence show that weathering of rock and biogenic uptake are tightly coupled in this fast weathering, kinetically-limited regime. In support of this rock-derived nutrient supply scenario we find that no bio-element except P and K becomes substantially recycled, i.e. re-mineralised ~~and re-utilised by recycling~~ from organic litter~~.~~ and then bio-utilised again. Instead, we infer that Mg~~ and~~, other ~~bio-~~nutrients and the plant beneficial element Si accumulate in a forest still growing after clear-cutting up to 50 years ago. As an alternative mechanism likely in operation in pre-forest management times we suggest that bio-utilised elements ~~are~~were disposed from the forest ecosystem in coarse woody debris (CWD) and Si in phytoliths eroded with leaf litter. ~~Today CWD is exported by logging. In pre-anthropogenic times, the same~~ CWD has potentially been eroded following tree death~~, during landslides, or~~ after wind throw~~.~~, or as ash after wildfires. We find that Mg is taken up from trees along the entire depth of the weathering profile down to ~~7~~6 m depth as indicated by the light Mg isotopic composition of the easily exchangeable soil fraction. Therefore we provide ~~the first direct observation that~~entirely novel means on how biota actively affects weathering fluxes. We ~~conclude~~suggest that in this kinetically-limited regime weathering is tightly coupled to rapid nutrient utilisation and erosion. Finally, we speculate that rapid nutrient erosion might be coupled to fast weathering globally. This coupling then is significant in geologically active mountains where CWD and bio-opal erosion is high and might present a hitherto underestimated solid export flux of elements previously released by chemical weathering.

~~7~~8 Appendices

Appendix A: Calculating δ^{26}Mg in bulk tree

We calculate the Mg isotopic composition of bulk tree ($\delta^{26}Mg_{tree}$) by a mass balance comprising the above-ground (needles, branches, stem) and belowground (roots) tree compartments. We measured δ^{26}Mg in foliage and stem wood. To estimate the isotopic composition of bulk *Pinus ponderosa* and *Pinus jeffrey* we combine these results with δ^{26}Mg and Mg concentration from ~~(~~Bolou-Bi et al~~.,~~. (2012) and the biomass of different compartments of *Pinus ponderosa* from (Laclau, 2003). We did not measure δ^{26}Mg in roots because of the challenges related to their purification from soil particles. Instead we use the published difference between δ^{26}Mg in roots and δ^{26}Mg in wood (Bolou-Bi et al., 2012) to infer δ^{26}Mg in roots from our measured value in wood. The isotopic composition of bulk tree is finally calculated by Eq. (A1), where $\mathrm{f}^{\mathrm{Mg}}_{\mathrm{compartment}}$ is the fraction of Mg in a given tree compartment.

$$\delta^{26}Mg_{bulk\ tree} = f^{Mg}_{needle} \cdot \delta^{26}Mg_{needle} + f^{Mg}_{stem} \cdot \delta^{26}Mg_{stem} + f^{Mg}_{root} \cdot \delta^{26}Mg_{root} \tag{A1}$$

The inferred isotopic composition of roots is 0.43 ‰ for *Pinus ponderosa* and 0.34 ‰ for *Pinus jeffrey*. The $\delta^{26}Mg_{tree}$ plotted in ~~Fig. 3~~Fig. 3 represents a mean value of bulk *Pinus ponderosa* and *Pinus jeffrey*.

Appendix B: X-ray diffraction analyses and the potential incorporation of Mg into secondary minerals

Powder X-ray diffraction analyses (Siemens D5000, Cu-Kα radiation) were performed for mineral identification on selected soil, saprolite and bedrock samples. Figure B1 indicates characteristic reflections for some major and minor minerals. Kaolinite is the only secondary mineral identified. The limit of detection is 5 %.

The absence of Mg-clays and the presence of kaolinite was confirmed by ~~a~~ published clay ~~content~~contents of less than 10 % in the soils (Dahlgren et al., 1997), and by thermodynamic modelling (PhreeqC). Because kaolinite has a low Mg content (<0.03 wt~~%) (~~%, Wimpenny et al., 2014) and a relatively low adsorption cation exchange capacity (CEC) of < 10 $\mathrm{cmol_c\ kg^{-1}}$

(Wimpenny et al., 2014) it is unlikely to incorporate Mg in such amounts that the Mg mass balance in soil is affected. Therefore, neoformation of Mg-clays is not the mechanism that preferentially removes ^{26}Mg from soil solution.

The fraction of Mg potentially contained in clay (f_{sec}^{Mg}) was calculated from the following mass balance. f_{sec}^{Mg} is governed by a mixture between Mg partitioned into Mg-clays and Mg partitioned into primary minerals such as biotite and amphibole. While the abundances of Mg-clays is at maximum 5 % (XRD limit of detection), primary minerals like biotite and amphibole are identified but not quantified by XRD. Hence, we estimate the relative abundances of biotite and amphibole from bedrock analysis (Bateman and Wones, 1972) which we consider to be applicable to soil too given the kinetically-limited weathering regime. We assume all mafic constituents to contain Mg. We use montmorillonite $(Al_{1.67}Mg_{0.33})[(OH)_2Si_4O_{10}]Na_{0.33}*H_2O$ (Harder, 1972) and biotite $K(Mg)_3[(OH,Fe)_2(Al,Fe,Ti)Si_3O_{10}]$ as model endmembers for Mg-clays and Mg carrying primary minerals, respectively. Applying the mineral Mg stoichiometry to the abundances of Mg-clays and biotite reveals that a Mg-clay content of 5 % in the soil translates into 4 % Mg partitioned into Mg-clays and 96 % Mg partitioned into biotite. This 4 % is used for f_{sec}^{Mg} in Eq. (1), which is solved for $\delta^{26}Mg_{sec}$ (see Sect. ~~3.2~~4.1).

This calculation confirms that the bulk soil sample with the highest measured δ^{26}Mg (-0.05 ‰), assuming it contains a maximum allowable Mg-clay content of 5 %, can only be explained if $\delta^{26}Mg_{sec}$ is +4.0 ‰, which is highly unlikely (Wimpenny et al., 2014 and references therein). Alternatively, if we use the maximum $\delta^{26}Mg_{sec}$ value observed for Mg-clay of 0.5 ‰ (Ryu et al., 2016 and references therein) in Eq. (1), then the Mg fraction in the bulk soil carried by Mg-clays (f_{sec}^{Mg}) were 24 %. This 24 % Mg partitioned into Mg-clays can be converted into a 30 % Mg-clay content in the bulk soil, which by far exceeds the XRD detection limit. Such high clay content was not observed by XRD (Fig. B1).

Finally, we explore whether Mg isotope fractionation by Mg adsorption onto kaolinite and amorphous hydroxides might result in the negative $\delta^{26}Mg_{diss}$. The evidence for Mg isotope fractionation during adsorption/desorption is not conclusive and is discussed in (Wimpenny et al., 2014 and references therein). Recent experimental evidence suggests that Mg adsorption is mostly associated with a slightly negative (-0.1 ‰) or complete absence of Mg isotope fractionation. Thus, our adsorbed Mg (termed ‘exchangeable’) likely reflects the isotopic composition of the fluid from which the exchange occurred. Indeed our isotopically light exchangeable Mg isotope analyses is virtually ~~identically~~identical to $\delta^{26}Mg_{diss}$.

Moreover, for such a process to shift δ^{26}Mg in the isotope mass balance (Eq. (1)), a substantial amount of Mg would need to be adsorbed. Our analyses of exchangeable Mg mass in regolith samples indicate that this compartment makes up less than 0.52 % of the bulk regolith sample (Table S1). This low mass is consistent with the low cation exchange capacity measured in Providence Creek soils (e.g., $Mg^{2+} < 0.45$ cmol$_c$ kg^{-1}, Johnson et al., 2011). Hence, neither clay formation nor adsorption is the mechanism that removes isotopically heavy Mg from soil solutions.

Appendix C: ~~Input~~Determining foliage, stem and root litter fall fluxes

Since litter data ~~to estimate~~for Providence Creek is not available we use total foliage litter fall fluxes of *Pinus ponderosa* from literature (Grady and Hart, 2006; Klemmedson et al., 1990; Law et al., 1999) and multiply its mean value (see Table S4c) with the elemental foliage litter concentration of *Pinus ponderosa* (Klemmedson et al., 1990) to determine L^{X}_{foliage} for K, Ca, Mg, P and Na. To determine L^{X}_{foliage} for Si we used L^{Si}_{foliage} data from Bartoli (1983) and simply converted the units. To determine L^{X}_{root} we used root litter production data from Röderstein et al. (2005). ~~and s~~Since roots were not sampled in this study we used Mg, Ca and K root concentrations from *Picea abies* (Bolou-Bi et al., 2012), ~~the~~ P root concentration from *Pinus sylvestris* (George et al., 1997), and ~~and the~~ Na and Si needle concentration from *Pinus ponderosa* from this study. We used Na and Si needle concentration instead its root concentrations as elemental needle and root concentrations are generally similar. Moreover, there is a lack of Na and Si root concentration for coniferous trees in the literature. To determine L^{X}_{trunk} we estimated the *Pinus ponderosa* minimum and maximum trunk wood biomass by using a logging calculator (www.burleyboys.com, for input parameters see below) and *Pinus ponderosa* Mg, Ca, K, Na and Si wood concentrations from this study and P wood concentration from *Pinus contorta* (Pearson et al., 1987).

To estimate a lower limit of *Pinus ponderosa* trunk wood biomass, we use a diameter at breast height (DBH) of 63 cm (Law et al., 1999), an upper diameter of 42 cm (by assuming that the diameter in the crown is reduced by one third compared to the DBH), a tree height of 34 m (Law et al., 1999), and a stand density of 40,000 trees per square kilometre. To convert the trunk wood biomass into an annual growing flux we used a living time of 250 years (Law et al., 1999). To estimate an upper limit of *Pinus ponderosa* trunk wood biomass we assume a younger forest (200 years) but denser (62,500 trees per square kilometre) forest stand.

~~8~~9 Author contributions

D.U. analysed samples, interpreted data, wrote text. J.S. conducted field work, analysed samples, interpreted data, wrote text. J.B. conducted field work, interpreted data, wrote text. J.D. conducted field work, provided background information. F.v.B. designed study, conducted field work, interpreted data, wrote text.

~~9~~10 Competing financial interests

The authors declare no competing financial interests.

~~10~~11 Additional information

Supplementary data tables are available in the online version of the paper.

~~11~~12 Acknowledgements

We thank R. Naumann (GFZ) for X-ray diffraction and X-ray fluorescence analyses. A. Gottsche (GFZ) is acknowledged for anion quantification using ion chromatography and for assistance in X-ray fluorescence analyses. We also thank R. Meyer (GFZ) for trace element (P) water analyses by Q-ICP-MS (iCAP-Q). Logistical support and discharge data was provided by the NSF-supported Southern Sierra Critical Zone Observatory: time-series water sampling, sample pre-treatment in the field and shipping was done by M. Meadows (University of California, Merced); C. Hunsacker (US Forest Service, Fresno) is thanked for field support and daily Providence Creek discharge data (http://criticalzone.org/sierra/data). We thank M. Oelze (GFZ), F. Lang (University of Freiburg~~) and~~), W. Wilcke (KIT, Karlsruhe), and D. Calmels (UPSud, Orsay) for discussions. D.U. and F.v.B. are grateful for funding by the German National Science Foundation priority Program 1685 "Ecosystem nutrition: forest strategies for limited phosphorus resources".

~~12~~13 References

Aciego, S. M., Riebe, C. S., Hart, S. C., Blakowski, M. A., Carey, C. J., Aarons, S. M., Dove, N. C., Botthoff, J. K., Sims, K. W. W. and Aronson, E. L: Dust outpaces bedrock in nutrient supply to montane forest ecosystems, Nat. Commun., 8, 14800, 2017.

Andrews, M. G., Jacobson, A. D., Lehn, G. O., Horton, T. W., and Craw, D.: Radiogenic and stable Sr isotope ratios (87Sr/86Sr, δ88/86Sr) as tracers of riverine cation sources and biogeochemical cycling in the Milford Sound region of Fiordland, New Zealand, Geochim. Cosmochim. Ac., 173, 284-303, 2016.

Arunachalam, J., Emons, H., Krasnodebska, H. and Mohl, C.: Sequential extraction studies on homogenized forest soil samples, Sci. Total Environ., 181, 147-159, 1996.

Bales, R. C., Hopmans, J. W., O'Geen, A. T., Meadows, M., Hartsough, P. C., Kirchner, P., Hunsaker, C. T. and Beaudette, D.: Soil moisture response to snowmelt and rainfall in a Sierra Nevada Mixed-Conifer forest, Vadose Zone J., 10, 786-799, 2011.

Bartoli, F.: The biogeochemical cycle of silicon in two temperate forest ecosystems, Ecol. Bull., 35, 469-476, 1983.

Bateman, P.C. and Wones, D.R.: Huntington Lake Quadrangle, Central Sierra Nevada, California - Analytical Data, Shorter Contributions to General Geology, Geological Survey Professional Paper 724-A, 1972.

Black, J. R., Epstein, E., Rains, W. D., Yin, Q.-Z. and Casey, W. H.: Magnesium-isotope fractionation during plant growth, Environ. Sci. Technol., 42, 7831-7836, 2008.

~~Bolou-Bi E.B., Poszwa, A., Leyval, C. and Vigier, N.: Experimental determination of magnesium isotope fractionation during higher plant growth, Geochim. Cosmochim. Acta., 74, 2523-2537, 2010.~~

Bolou-Bi, E. B., Vigier, N., Poszwa, A., Boudot, J. P., and Dambrine, E.: Effects of biogeochemical processes on magnesium isotope variations in a forested catchment in the Vosges Mountains (France), Geochim. et Cosmochim. Acta, 87, 341-355, 2012.

Formatiert: Englisch (Vereinigte Staaten)

Bonan, G.B.: Forests and climate change: forcings, feedbacks, and the climate benefits of forests, Science, 320, 1444-1449, 2008.

Bouchez, J., von Blanckenburg, F. and Schuessler, J. A.: Modelling novel stable isotopes in the weathering zone, Am. J. Sci., 313, 267-308, 2013.

Boy, J., and Wilcke, W.: Tropical Andean forest derives calcium and magnesium from Saharan dust, Global Biogeochem. Cy., 22, 2008.

Brantley, S. L. and Lebedeva, M.: Learning to Read the Chemistry of Regolith to Understand the Critical Zone, Annu. Rev. Earth Pl. Sc., 39, 387-416, 2011.

Brantley, S. L., Megonigal, J. P., Scatena, F. N., Balogh-Brunstad, Z., Barnes, R. T., Bruns, M. A., Van Cappellen, P., Dontsova, K., Hartnett, H. E., Hartshorn, A. S., Heimsath, A., Herndon, ~~-~~E., Jin, L., Keller, C. K., Leake, J . R., McDowell, W. H., Meinzer, F. C., Mozdzer, T. J ., Petsch, S., Pett-Ridge, J., Pregitzer, K. S., Raymond, P. A., Riebe, C. S., Shumaker, K., Sutton-Grier, A., Walter, R. and Yoo, K.: Twelve testable hypotheses on the geobiology of weathering, Geobiology, 9, 1-26, 2011.

Bullen, T. and Chadwick, O.: Ca, Sr and Ba stable isotopes reveal the fate of soil nutrients along a tropical climosequence in Hawaii. Chem. Geol., 422, 25-45, 2016.

Burley Boys: http://www.burleyboys.com, last access: 23th November 2016

Chapela Lara, M~~.,~~., Buss, H. L., Pogge von Strandmann, P. A. E., Moore, O. W. and Schuessler, J. A.: The influence of critical zone processes on the Mg isotope budget in a tropical, highly weathered andesitic catchment, Geochim. Cosmochim. ~~Cosmoch.f Ac., 2016, in revision~~Ac., 202, 77-100, 2017.

Clymans, W., Conley, D. J., Battles, J. J., Frings, P. J., Koppers, M. M., Likens, G. E., and Johnson, C. E.: Silica uptake and release in live and decaying biomass in a northern hardwood forest, Ecology, 97, 3044-3057, 2016.

Cornelis, J. T., Ranger, J., Iserentant, A., and Delvaux, B.: Tree species impact the terrestrial cycle of silicon through various uptake, Biogeochemistry, 97, 231-245, 2010.

Critical Zone: http://criticalzone.org/sierra/data/datasets, last access: 15th November 2016

Dahlgren, R. A., Boettinger, J. L., Huntington, G. L. and Amundson, R. G.: Soil development along an elevational transect in the western Sierra Nevada, California, Geoderma, 78, 207-236, 1997.

Dixon, J. L., Heimsath, A. M. and Amundson, R.: The critical role of climate and saprolite weathering in landscape evolution, Earth Surf. Proc. Land., 34, 1507-1521, 2009.

Dixon. J. L. and von Blanckenburg, F.: Soils as pacemakers and limiters of global silicate weathering, C. ~~-~~R. Geosci., 344, 597-609, 2012.

Eagan, S. M., Hunsaker, C. T., Dolanc, C. R., Lynch, M. E. and Johnson, C. R.: Discharge and Sediment Loads at the Kings River Experimental Forest in the Southern Sierra Nevada of California, 2007.

~~Fantle, M. S. and Tipper, E. T.: Calcium isotopes in the global biogeochemical Ca cycle: Implications for development of a Ca isotope proxy, Earth Sci. Rev., 129, 148–177, 2014.~~

Formatiert: Englisch (Vereinigte Staaten)

Fraysse, F., Pokrovsky, O. S., Schott, J. and Meunier, J.-D.: Surface chemistry and reactivity of plant phytoliths in aqueous solutions, Chem. Geol., 258, 197-206, 2009.

Frings, P. J., Clymans, W., Fontorbe, G., De La Rocha, C. L. and Conley, D. J.: The continental Si cycle and its impact on the ocean Si isotope budget, Chem.Geol., 425, 12-36, 2016.

Galy, A., Yoffe, O., Janney, P. E., Williams, R. W., Cloquet, C., Alard, O., Halicz, L., Wadhwa, M., Hutcheon, I. D., Ramon, E. and Carignan, J.: Magnesium isotope heterogeneity of the isotopic standard SRM980 and new reference materials for magnesium-isotope-ratio measurements, J. Anal. At. Spectrom., 18, 1352–1356, 2003.

Galy, V., Peucker-Ehrenbrink, B. and Eglington, T.: Global carbon export from the terrestrial biosphere controlled by erosion, Nature, 521, 204-207, 2015.

George, E., Seith, B., Schaeffer, C., and Marschner, H.: Responses of Picea, Pinus and Pseudotsuga roots to heterogeneous nutrient distribution in soil, Tree Physiol., 17, 39-45, 1997.

Grady, K. C. and Hart, S. C.: Influences of thinning, prescribed burning, and wildfire on soil processes and properties in southwestern ponderosa pine forests: a retrospective study, For. Ecol. Manag., 234, 123-135, 2006.

Graham, -R. T. and Jain, T. B.: Ponderosa Pine Ecosystems, USDA Forest Service Gen. Tech. Rep., PSW-GTR-198, 2005.

Hahm, W. J., Riebe, C. S., Lukens, C. E. and Araki, S.: Bedrock composition regulates mountain ecosystems, P. Natl. Acad. Sci. USA, 111, 3338-3343, 2014.

Harder, H.: The role of magnesium in the formation of smectite mineral,. Chem. Geol, 10, 31-39, 1972.

Jobbagy, E. G. and Jackson R.B.: The distribution of soil nutrients with depth: Global patterns and the imprint of plants, Biogeochemistry, 53, 51-77, 2001.

Hilton, R. G.: Climate regulates the erosional carbon export from the terrestrial biosphere: Geomorphology, 277, 118-132, 2017.

Johnson, C. M., Beard, B. L. and Albarède, F.: Geochemistry of Non-Traditional Stable Isotopes, Rev. Mineral. Geochem., 55, 2004.

Johnson, C. E., Siccama, T. G., Denny, E. G., Koppers, M. M. and Vogt, D. J.: In situ decomposition of northern hardwood tree boles: decay rates and nutrient dynamics in wood and bark, Can. J. Forest Res., 44, 1515-1524, 2014.

Johnson, D.W., Hunsaker, C.T., Glass , D.W., Rau, B.M. and Roath, B.A.: Carbon and nutrient contents in soils from the Kings River Experimental Watersheds, Sierra Nevada Mountains, California, Geoderma, 160, 490-502, 2011.

Jongmans, A.G., van Breemen, N., Lundström, U., van Hees, P. A. W., Finlay, R. D., Srinivasan, M., Unestam, T., Giesler, R., Melkerud, P.-A. and Olsson, M.: Rock-eating fungi, Nature, 389, 682-683, 1997.

Kirchner, J. W., Finkel, R. C., Riebe, C. S., Granger, D. E., Clayton, J. L., King, J. G., and Megahan, W. F.: Mountain erosion over 10 yr, 10 k.y., and 10 m.y. time scales. Geology 29, 591–594 (2001).

Klemmedson, J. O., Meier, C. E. and Campbell, R. E.: Litter fall transfers of dry matter and nutrients in ponderosa pine stands, Can. J. Forest Res., 20, 1105-1115, 1990.

Klemmedson, J. O.: Decomposition and nutrient release from mixtures of Gambel oak and ponderosa pine leaf litter, Forest Ecol. Manag., 47, 349-361, 1992.

Laclau, P.: Biomass and carbon sequestration of ponderosa pine plantations and native cypress forests in northwest Patagonia, Forest Ecol. Manag., 180, 317-333, 2003.

Landeweert, R., Hoffland, E., Finlay, R. D., Kuyper, T. W. and van Breemen, N.: Linking plants to rocks: ectomycorrhizal fungi mobilize nutrients from minerals, TRENDS Ecol. Evol., 16, 248-254, 2001.

Lang, F., Bauhus, J., Frossard, E., George, E., Kaiser, K., Kaupenjohann, M., Krüger, J., Matzner, E., Polle, A., Prietzel, J., Rennenberg, H. and Wellbrock, N.: Phosphorus in forest ecosystems: New insights from an ecosystem nutrition perspective, J. Plant Nutr. Soil Sc., 179, 129-135, 2016.

Law, B. E., Ryan, M. G. and Anthoni, P. M.: Seasonal and annual respiration of a ponderosa pine ecosystem, Glob. Change Biol., 5, 169-182, 1999.

Lucas, Y.: The role of plants in controlling rates and products of weathering: Importance of biological pumping, Annu. Rev. Earth Pl. Sc., 29, 135-163, 2001.

Ma, L., Teng, F. Z., Jin, L., Ke, S., Yang, W., Gu, H. O. and Brantley, S. L.: Magnesium isotope fractionation during shale weathering in the Shale Hills Critical Zone Observatory: Accumulation of light Mg isotopes in soils by clay mineral transformation, Chem. Geol., 397, 37-50, 2015.

~~Mahowald, N. M., Baker, A.R., Bergametti, G., Brooks, N., Duce, R.A., Jickells, T.D., Kubilay, N., Prospero, J.~~Marschner, H: Marschner's mineral nutrition of higher plants, Academic press, 2011.

~~M., and Tegen, I. Atmospheric global dust cycle and iron inputs to the ocean. Global Biogeochemical Cycles, 19, 2005.~~

Mavromatis, V., Prokushkin, A. S., Pokrovsky, O. S., Viers, J. and Korets, M. A.: Magnesium isotopes in permafrost-dominated Central Siberian larch forest watersheds, Geochim. Cosmochim. Ac., 147, 76-89, 2014.

McCorkle, E. M., Berhe, A. A., Hunsaker, C. T., Johnson, D. W., McFarlane, K. J., Fogel, M. L. and Hart, S. C.: Tracing the source of soil organic matter eroded from temperate forest catchments using carbon and nitrogen isotopes, Chem. Geol., 44, 172-184, 2016.

Meng-Ning, D. A. I., Zhi-An, B. A. O., Kai-Yun, C. H. E. N., and Hong-Lin, Y. U. A. N.: In situ Analysis of Mg Isotopic Compositions of Basalt Glasses by Femtosecond Laser Ablation Multi-collector Inductively Coupled Plasma Mass Spectrometry, Chinese J. Anal. Chem., 44, 173-178, 2016.

Moulton, K. L., West, J. and Berner, R. A.: Solute flux and mineral mass balance approaches to the quantification of plant effects on silicate weathering, Am. J. Sci., 300, 539–570, 2000.

Oeser, M., Wexer, S., Horn, I., and Schuth, S.: High-Precision Fe and Mg Isotope Ratios of Silicate Reference Glasses Determined In Situ by Femtosecond LA-MC-ICP-MS and by Solution Nebulisation MC-ICP-MS, Geostand. Geoanal. Res., 38, 311-328, 2014.

Opfergelt, S~~. and Delmelle, P.: Silicon isotopes and continental weathering processes: Assessing controls on Si transfer to the ocean, C. R. Geosci., 344, 723-738, 2012.~~

Formatiert: Schriftart: 11 Pt.

Formatiert: Schriftart: 11 Pt.

~~Opfergelt, S.~~, Burton, K.W., Georg, R.B., West, A.J., Guicharnaud, R.A., Sigfusson, B., Siebert, C., Gislason, S.R. and Halliday, A.N.: Magnesium retention on the soil exchange complex controlling Mg isotope variations in soils, soil solutions and vegetation in volcanic soils, Iceland, Geochim. Cosmochim. Ac., 125, 110-130, 2014.

Pearson, J. A., Knight, D. H., and Fahey, T. J.: Biomass and nutrient accumulation during stand development in Wyoming lodgepole pine forests, Ecology, 68, 1966-1973, 1987.

Pogge von Strandmann, P.A.E., Elliott, T., Marschall, H. R., Coath, C., Lai, Y.-J., Jeffcoate, A. B. and Ionov, D. A.: Variations of Li and Mg isotope ratios in bulk chondrites and mantle xenoliths. Geochim. Cosmochim. Ac., 75, 5247-5268, 2011.

Porder, S., Vitousek, P. M., Chadwick, O. A., Chamberlain, C. P. and Hilley, G. E.: Uplift, Erosion and Phosphorus Limitation in Terrestrial Ecosystems, Ecosystems, 10, 158-170, 2007.

Riebe, C.S., Kirchner, J.W. and Finkel, R.C.: Long-term rates of chemical weathering and physical erosion from cosmogenic nuclides and geochemical mass balance, Geochim. Cosmochim. Ac., 67, 4411-4427, 2003.

Riebe, C. S. and Granger, D. E.: Quantifying effects of deep and near-surface chemical erosion on cosmogenic nuclides in soils, saprolite, and sediment, Earth Surf. Proc. Land., 38, 523-533, 2013.

Röderstein, M., Hertel, D. and Leuschner, C.: Above-and below-ground litter production in three tropical montane forests in southern Ecuador, J. Trop. Ecol., 21, 483-492, 2005.

Roering, J. J., Marshall, J., Booth, A. M., Mort, M. and Jin, Q. S.: Evidence for biotic controls on topography and soil production, Earth Planet. Sc. Lett., 298, 183-190, 2010.

Ryu, J.-S., Vigier, N., Decarreau, A., Lee, S.-W., Le, K.-S., Song, H. and Petit, S.: Experimental investigation of Mg isotope fractionation during mineral dissolution and clay formation, Chem. Geol., 445, 135-145, 2016.

Schaller, M., von Blanckenburg, F., Hovius, N., and Kubik, P.: Large-scale erosion rates from in situ-produced cosmogenic nuclides in European river sediments, Earth Planet. Sc. Lett, v. 188, no. 3-4, p. 441-458, 2001.

Schuessler, J. A., and von Blanckenburg, F.: Testing the limits of micro-scale analyses of Si stable isotopes by femtosecond laser ablation multicollector inductively coupled plasma mass spectrometry with application to rock weathering, Spectrochim. Acta B, 98, 1-18, 2014.

Schuessler, J. A., Kämpf, H., Koch, U., Alawi, M.: Earthquake impact on iron isotope signatures recorded in mineral spring water. Journal of Geophysical Research: Solid Earth, 121, 2016. doi:10.1002/2016JB013408

Sommer, M., Jochheim, H., Höhn, A., Breuer, J., Zagorski, Z., Busse, J., and Kaczorek, D.: Si cycling in a forest biogeosystem–the importance of transient state biogenic Si pools, Biogeosciences, 10, 4991-5007, 2013.

Stone, E. L. and Kalisz, P. J.: On the maximum extent of tree roots, For. Ecol. Manag., 46, 59-102, 1991.

Tipper, E.T., Lemarchand, E., Hindshaw, R.S., Reynolds, B.C. and Bourdon, B.: Seasonal sensitivity of weathering processes: hints from magnesium isotopes in a glacial stream, Chem. Geol., 312-313, 80-92, 2012.

Vitousek, P. M. and Farington, H.: Nutrient limitation and soil development: Experimental test of a biogeochemical theory, Biogeochemistry, 37, 63-75, 1997.

~~Wang, K., and Jacobsen, S. B.: An estimate of the Bulk Silicate Earth potassium isotopic composition based on MC-ICPMS measurements of basalts, Geochim. Cosmochim. Ac., 178, 223-232, 2016.~~

West, A.J., Galy, A. and Bickle, M.J.: Tectonic and climatic controls on silicate weathering, Earth Planet. Sc. Lett., 235, 211-228, 2005.

Wimpenny, J., Colla, C. A., Yin, Q.-Z., Rustad, J. R. and Casey, W. H.: Investigating the behavior of Mg isotopes during the formation of clay minerals, Geochim. Cosmochim. Ac., 128, 178-194, 2014.

Formatiert: Schriftart: +Textkörper (Calibri)

~~13~~14 Tables

Tab. 1: Glossary of symbols

	Total mass fluxes (e.g. in t km^{-2} yr^{-1})
D	Denudation rate; i.e the sum of chemical and physical denudation; Eq. (7); Sect. 4.4
	Elemental fluxes F^X (e.g. in mol km^{-2} yr^{-1})
RP^X	Regolith production flux of element X; transfer of X from bedrock to regolith at the weathering front; Eq. (7); Sect. 4.4
W^X_{river}	Dissolved river flux of element X; Eq. (6); Sect. 4.4
$W^X_{regolith}$	Net solubilisation flux of element X; release flux of X from minerals minus the flux of incorporation of X into secondary minerals; Eq. (9); Sect. 4.5
L^X	Litter fall flux of element X; sum of leaf, trunk and root litter flux of X from trees to topsoil through litter fall; Eq. (14); Sect. 4.7
E^X_{org}	Erosion flux of element X in particulate organic matter or phytoliths; Eq. (4); Sect. 4.2
	Normalised elemental fluxes f^X
$w^X_{isotope}$	Dissolved export flux of element X relative to the regolith production flux of element X, calculated from isotopes; Eq. (5); sect. 4.3
w^X_{river}	Dissolved export flux of element X relative to the regolith production flux of element X, calculated from river loads; W^X_{river} / RP^X; Eq. (8), Sect. 4.4
$w^X_{regolith}$	Normalised net solubilisation flux of element X; $W^X_{regolith}$ / RP^X; Eq. (11), Sect. 4.5
DEE^X	Dissolved export efficiency of element X; W^X_{river} / $W^X_{regolith}$; Eq. (12), Sect. 4.6
DEE^X_{Na}	Dissolved export efficiency of element X; Na-normalised W^X_{river} / $W^X_{regolith}$; Eq. (13), Sect. 4.6
Rec^X	Nutrient recycling factor; number of passages X takes through the vegetation after its initial release from rock; L^X/ $W^X_{regolith}$; Eq. (14), Sect. 4.7
	Elemental mass fractions
f^{Mg}_{sec}	Fraction of Mg carried by secondary minerals relative to total soil Mg; Eq. (1), Sect. 4.1
f^{Mg}_{uptake}	Fraction of Mg taken up by plants relative to Mg available in soil solution; Eq. (2), Sect. 4.2
τ^X_{Zr}	Loss fraction of element X; elemental loss or gain relative to unweathered bedrock; Eq. (10); Sect. 4.5
	Mg stable isotope properties (in ‰)
$\delta^{26}Mg_{comp.}$	Normalised ^{26}Mg/^{24}Mg isotope ratio in compartments (e.g. rock, sec, diss, reg, sed, topsoil, plant)
$\Delta^{26}Mg_{plant-diss}$	Isotope fractionation factoric difference between Mg in plants and dissolved Mg in soil water

Formatierte Tabelle

15 Figures

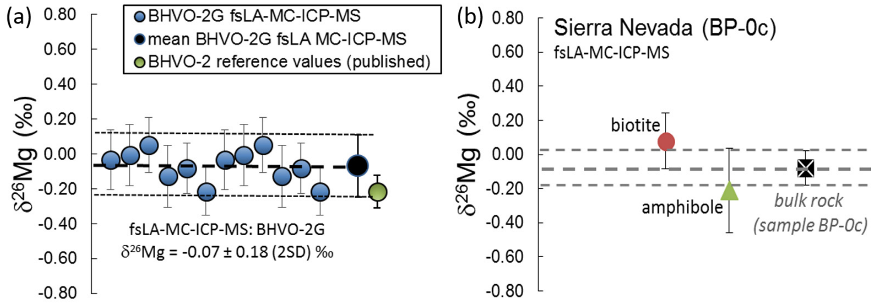

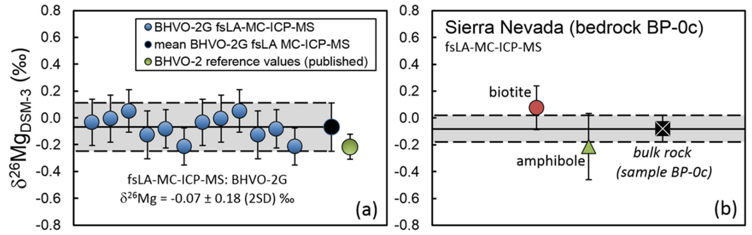

Fig. ~~1:~~1: Mg isotopic composition measured by fsLA-MC-ICP-MS. *(a): Repeat measurements of BHVO-2G. Solid black circle and bold dashed line repesents mean value of all BHVO-2G measurements with the 2SD range resprented by stippled lines. Published literature data (Meng-Ning et al., 2016) is shown for comparison. (b): Biotite and amphibole of sample BP-0c measured by fsLA-MC-ICP-MS. Bulk rock is measured by solution MC-ICP-MS.*

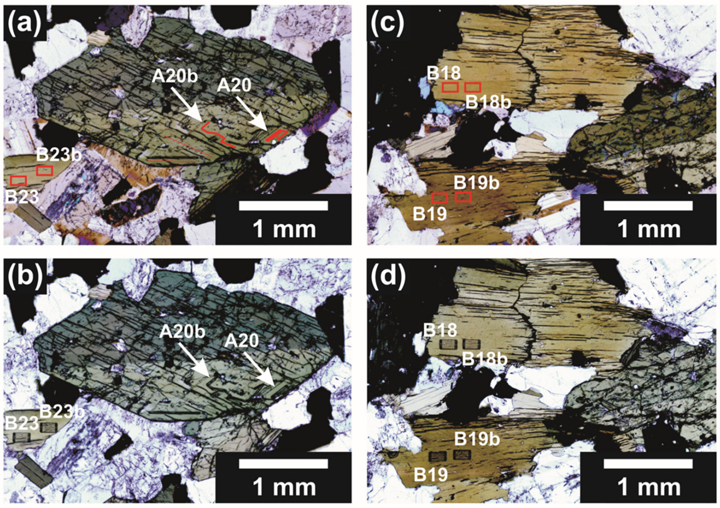

Fig. ~~2:~~2: Photomicrographs before and after fsLA-MC-ICP-MS. *Red rectangles and lines indicate laser ablation locations. Amphibole before (a) and after (b) fsLA-MC-ICP-MS. Biotite before (c) and after (d) fsLA-MC-ICP-MS.*

Formatiert: Zeilenabstand: einfach

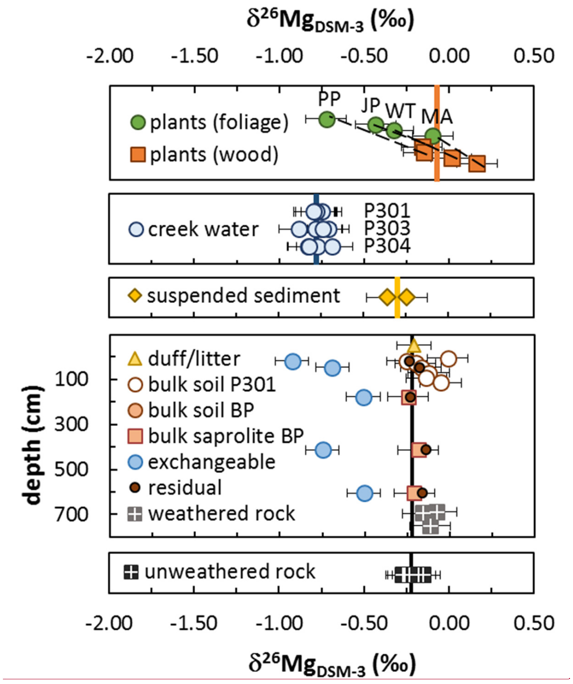
δ26MgDSM-3 (‰)
-2.00
-1.50
-1.00
-0.50
0.00
0.50
PP
JP
WT
MA
plants (foliage)
plants (wood)
creek water
P301
P303
P304
suspended sediment
duff/litter
bulk soil P301
bulk soil BP
bulk saprolite BP
exchangeable
residual
weathered rock
depth (cm)
100
300
500
700
unweathered rock

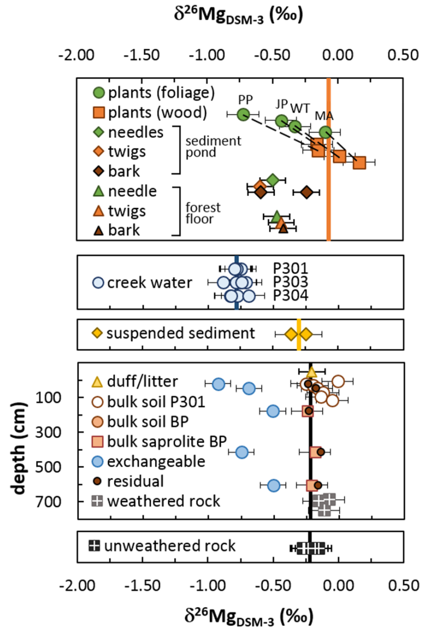

***Fig. ~~3:~~3:* Magnesium isotopic composition of the compartments at Providence Creek, Southern Sierra Nevada, USA.** *Vertical lines represent mean δ^{26}Mg values of bulk unweathered rock (black), bulk suspended sediment (yellow), bulk tree (orange, mass balance see Appendix C), and creek water (blue). The diagonal stippled lines connect woody with non-woody plant material of the same sample. Exchangeable and residual refer to~~:~~ sequentially extracted soil phases~~:~~. P301, P303, P304~~:~~ refer to headwater catchments at Providence Creek~~:~~. BP~~:~~ refers to the soil-saprolite profile (Balsam Profile)~~:~~. PP refers to~~:~~ Ponderosa Pine [Pinus ponderosa],~~:~~ JP~~:~~ refers to Jeffrey Pine [Pinus jeffreyi]~~:~~, WT refers to~~:~~ Whitethorn [Ceanothus cordulatus~~];~~], MA refers to~~:~~ Manzanita [Arctostaphylos manzanita]. Error bars amount to~~:~~ 0.10 ‰ (2SD).*

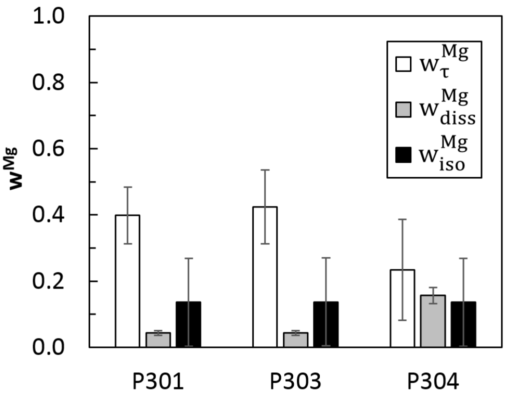

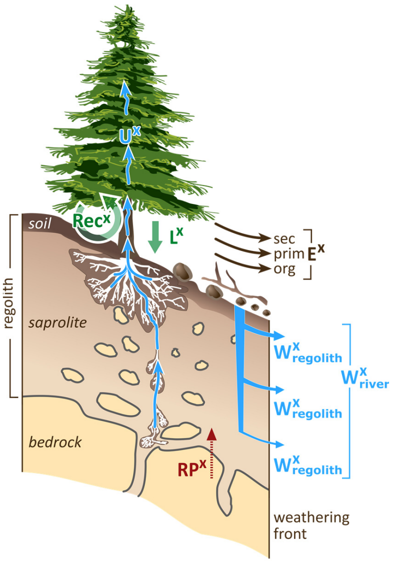

Fig.* ~~4:~~*4: Schematic figure illustrating the metrics used in our flux model. *"Org" refers to the sum of coarse woody debris (CWD), litter and trunk wood erosion. Rec*^{X} *refers to the nutrient recycling factor of element X, U*^{X} *refers to the nutrient uptake flux of element X, L*^{X} *refers to the litter flux of element X, RP*^{X} *refers to the regolith production flux of element X,* W_{river}^X *refers to the dissolved river flux of element X,* $W_{regolith}^X$ *refers to the net solubilisation flux of element X.*

Formatiert: Schriftart: Kursiv

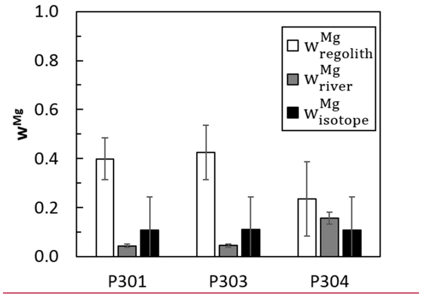

Fig. 5: ***Comparison of the relative weathering flux derived from Mg isotopes (~~w^{Mg}_{iso}~~$w^{Mg}_{isotope}$, Table S4b), dissolved river loads (~~w^{Mg}_{diss}~~w^{Mg}_{river}, Table S4b), and net solubilisation fluxes (~~w^{Mg}_{r}~~$w^{Mg}_{regolith}$, Table S4b) for the individual Providence Creek sub-catchments.*** *The ca. fourfold higher* ~~w^{Mg}_{diss}~~w^{Mg}_{river} *of the smallest watershed P304 compared to the larger watersheds P301 and P303 might be the result of the relatively high discharge record caused by higher baseflow (Eagan et al., 2007) for such a small watershed. For that reason we consider this catchment to be unrepresentative.*

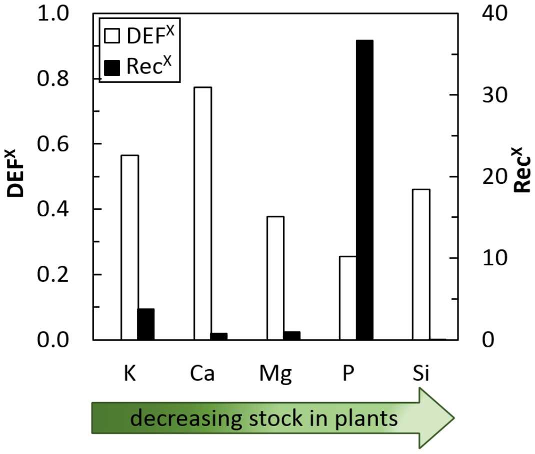

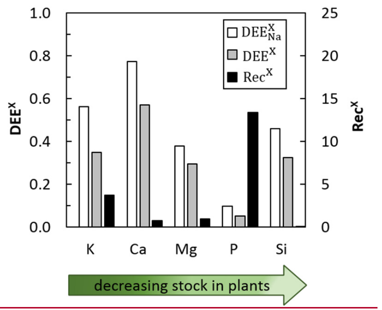

***Fig. ~~5:~~6: Dissolved export ~~fraction (DEF^X~~efficiency (DEE^X, left Y-axis, Table S4d - S4e) and nutrient recycling factor (Rec^X, right Y-axis, Table ~~S4e~~S4f) for macronutrients and the plant beneficial element Si**. The ~~DEF^X (Eq. (11))~~DEE^X quantifies the dissolved riverine loss of X from the ecosystem relative to its net release from the regolith. ~~The Rec^X (Eq. (12~~DEE^X refers to the pure ratio $W^X_{river}/W^X_{regolith}$ (Eq. (12)). DEE^X_{Na} refers to the ratio $W^X_{river}/W^X_{regolith}$ normalised over its corresponding Na-fluxes (Eq. (13)). Rec^X (Eq. (14)) quantifies how often an element X is bio-utilised by plants after its release by chemical weathering.*

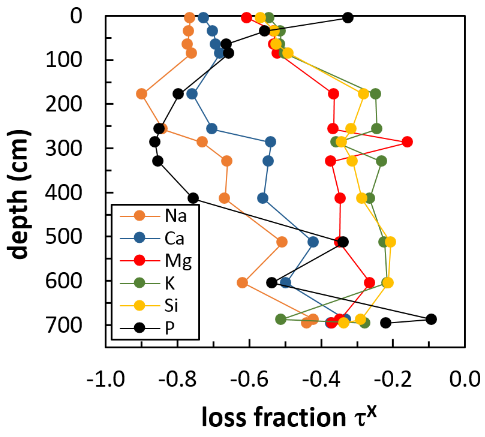

***Fig 7:* Loss fraction (τ^X) for macronutrients, the plant essential element Si, and Na of the soil-saprolite depth profile BP.** *A τ value < 0 indicates elemental loss in soil/saprolite relative to unweathered bedrock.*

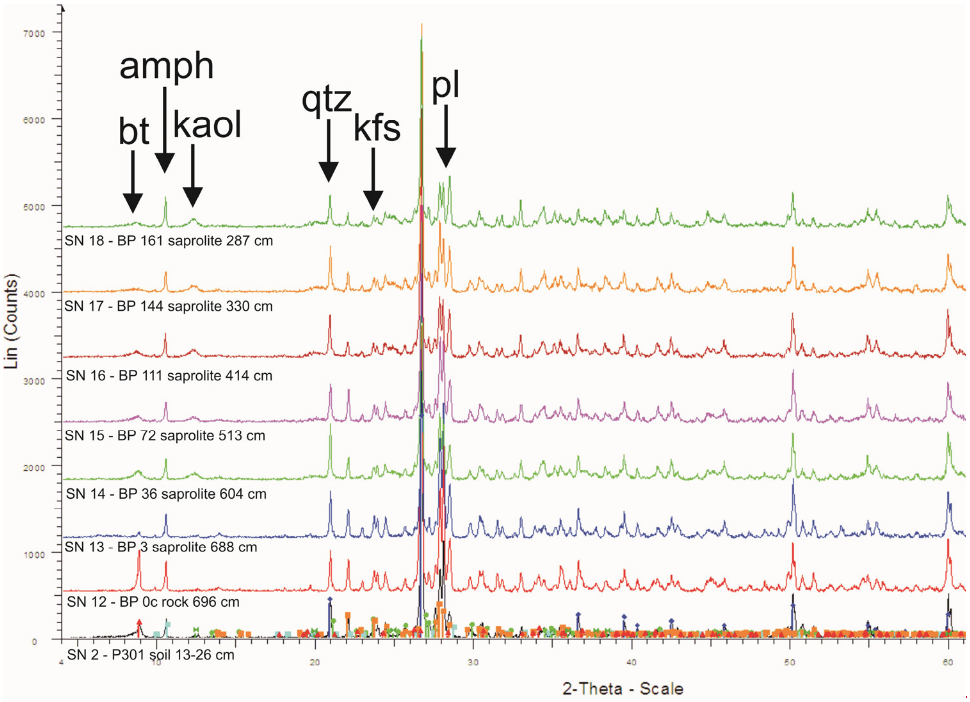
amph
bt
kaol
qtz
kfs
pl
Lin (Counts)
7000
6000
5000
4000
3000
2000
1000
0
SN 18 - BP 161 saprolite 287 cm
SN 17 - BP 144 saprolite 330 cm
SN 16 - BP 111 saprolite 414 cm
SN 15 - BP 72 saprolite 513 cm
SN 14 - BP 36 saprolite 604 cm
SN 13 - BP 3 saprolite 688 cm
SN 12 - BP 0c rock 696 cm
SN 2 - P301 soil 13-26 cm
4
10
20
30
40
50
60
2-Theta - Scale

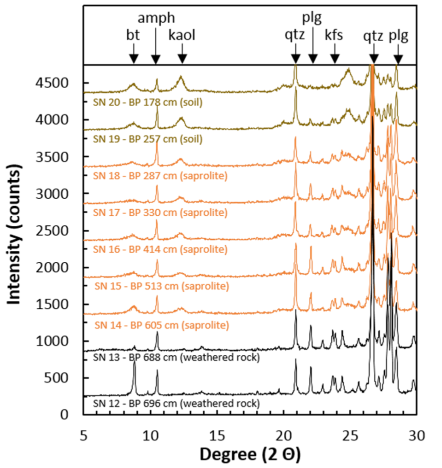

Fig. B1: X-ray diffraction (XRD) ~~pattern~~patterns of bulk soil, bulk saprolite, and bulk bedrock~~.~~ stacked on top of each other. *Major reflections of primary minerals (bt = biotite, amph = amphibole, qtz = quartz, kfs = K-feldspar, ~~pl~~plg = plagioclase) and secondary minerals (kaol = kaolinite) are indicated.*

Formatiert: Zeilenabstand: einfach